

DESIGN OF EFFICIENT BLUE PHOSPHORESCENT
BOTTOM EMITTING LIGHT EMITTING DIODES BY
MACHINE LEARNING APPROACH

MUHAMMAD ASYRAF BIN JANAI

FACULTY OF SCIENCE
UNIVERSITY OF MALAYA
KUALA LUMPUR

2019

**DESIGN OF EFFICIENT BLUE PHOSPHORESCENT
BOTTOM EMITTING LIGHT EMITTING DIODES BY
MACHINE LEARNING APPROACH**

MUHAMMAD ASYRAF BIN JANAI

**DISSERTATION SUBMITTED IN FULFILMENT OF
THE REQUIREMENTS FOR THE DEGREE OF MASTER
OF SCIENCE**

**DEPARTMENT OF PHYSICS
FACULTY OF SCIENCE
UNIVERSITY OF MALAYA
KUALA LUMPUR**

2019

UNIVERSITY OF MALAYA

ORIGINAL LITERARY WORK DECLARATION

Name of Candidate: **MUHAMMAD ASYRAF BIN JANAI**

Matric No: **SMA170033**

Name of Degree: **MASTER OF SCIENCE**

Title of Project Paper/Research Report/Dissertation/Thesis (“this Work”):

DESIGN OF EFFICIENT BLUE PHOSPHORESCENT BOTTOM EMITTING LIGHT EMITTING DIODES BY MACHINE LEARNING APPROACH

Field of Study: **THEORETICAL AND COMPUTATIONAL CHEMISTRY**

I do solemnly and sincerely declare that:

- (1) I am the sole author/writer of this Work;
- (2) This Work is original;
- (3) Any use of any work in which copyright exists was done by way of fair dealing and for permitted purposes and any excerpt or extract from, or reference to or reproduction of any copyright work has been disclosed expressly and sufficiently and the title of the Work and its authorship have been acknowledged in this Work;
- (4) I do not have any actual knowledge nor do I ought reasonably to know that the making of this work constitutes an infringement of any copyright work;
- (5) I hereby assign all and every rights in the copyright to this Work to the University of Malaya (“UM”), who henceforth shall be owner of the copyright in this Work and that any reproduction or use in any form or by any means whatsoever is prohibited without the written consent of UM having been first had and obtained;
- (6) I am fully aware that if in the course of making this Work I have infringed any copyright whether intentionally or otherwise, I may be subject to legal action or any other action as may be determined by UM.

Candidate’s Signature

Date: 11/7/2019

Subscribed and solemnly declared before,

Witness’s Signature

Date: 11/7/2019

Name:

Designation:

DESIGN OF EFFICIENT BLUE PHOSPHORESCENT BOTTOM EMITTING LIGHT EMITTING DIODES BY MACHINE LEARNING APPROACH

Abstract

This research aims to increase the efficiency of blue phosphorescent light-emitting diode (PhOLED) through machine learning models. Historical data from papers published prior to this research are used to train such model. From the model built, we are able to predict the current efficiency of PhOLED from a combination of materials parameters used in a device. Furthermore, the result of this research allows us to quantify the parameter of devices and rank them according to the feature importance. The feature importance describes the impact of any single parameter in a device based on the model and how it affects the device efficiency. The result of our experiment shows that Random Forest, a machine learning algorithm, produces the best fit to our dataset and hence able to make the most accurate prediction of device efficiency. This algorithm is then used to study the complex relationship of device features and efficiencies. It is found from the algorithm that triplet energy of electron transport layer is the most important feature in determining device efficiency among other features.

Keywords: PhOLED, Machine learning, Random forest, Efficiency

**REKA BENTUK DIOD PEMANCAR CAHAYA PHOSPHORESCENT BIRU
BERKECEKAPAN TINGGI MENGGUNAKAN KAEDAH PEMBELAJARAN
MESIN**

Abstrak

Penyelidikan ini bertujuan untuk meningkatkan tahap kecekapan peranti diod pemancar cahaya organik pendarfosfor (PhOLED) biru dengan menggunakan model pembelajaran mesin. Data daripada jurnal serta kertas penyelidikan yang telah diterbitkan sebelum penyelidikan ini ditulis telah digunakan untuk mengajar model tersebut. Daripada model yang telah dibina, kami berupaya untuk meramal kecekapan peranti PhOLED menggunakan kombinasi parameter bahan yang digunakan. Tambahan pula, model ini dapat membantu mengukur parameter dalam sesebuah peranti dan mengatur parameter tersebut berdasarkan darjah kepentingan. Darjah kepentingan sesuatu parameter memberi gambaran tentang impak yang diberi terhadap kecekapan peranti. Hasil kajian kami mendapati hutan rawak, satu algoritma pembelajaran mesin, menghasilkan ramalan yang terbaik dikalangan algoritma-algoritma yang digunakan. Kemudiannya, hutan rawak turut digunakan untuk penyelidikan yang lebih lanjut. Kami turut mendapati bahawa tenaga triplet untuk lapisan pengangkut elektron, mempunyai sumbangan yang terbesar dalam menentukan tahap kecekapan peranti.

Kata kunci: PhOLED, Pembelajaran mesin, Random forest, Kecekapan

ACKNOWLEDGEMENTS

I would like to thank my research and master's supervisor Assoc. Prof. Dr. Woon Kai Lin, who has guided me through this path, igniting my interest in this topic in particular. We kept going through different ideas for my research topic, from perovskite LED to programming and lastly machine learning and data science. I was given trust to study a field which is relatively new to me at that moment, up until I am able to finish this research. I must also thank my co supervisor, Assoc. Prof. Dr. Chan Chee Seng, who guided this research, especially in machine learning and artificial intelligence areas, where I had no prior experience on the matter.

Special thanks to my family for supporting physically and mentally throughout my time as a postgraduate student. They also encouraged me to never give up on my studies even at times, I felt like giving up halfway considering the problems and difficulties faced. Thanks to them, I managed to get to this point.

I am thankful for LDMRC lab members who helped me learning the ropes around the laboratories. They taught me a lot on how to use the machines, materials and lab equipment for my research, especially Wong Wah Seng and Arif. Thank you everybody, much appreciated.

TABLE OF CONTENTS

ORIGINAL LITERARY WORK DECLARATION	ii
ABSTRACT	iii
ABSTRAK	iv
ACKNOWLEDGEMENTS	v
TABLE OF CONTENTS	vi
LIST OF FIGURES	ix
LIST OF TABLES	xi
LIST OF SYMBOLS AND ABBREVIATIONS	xii
LIST OF APPENDICES	xiv
CHAPTER 1: INTRODUCTION	1
1.1 Introduction.....	1
1.2 Problem statement.....	1
1.3 Motivation and objectives.....	2
1.4 Outline for dissertation.....	3
CHAPTER 2: LITERATURE REVIEW	5
2.1 Organic Light-Emitting Diode (OLED).....	5
2.2 Working principles and parameters of OLED.....	9
2.2.1 Emitting layer.....	9
2.2.2 Anode and injection/buffer layer.....	11
2.2.3 Cathode and injection/buffer layer.....	12
2.2.4 Transport layer.....	13
2.3 Phosphorescent Organic Light-Emitting Diode (PhOLED).....	14
2.4 Device efficiency.....	15

2.5	Blue PhOLED limitations.....	17
CHAPTER 3: MACHINE LEARNING.....		19
3.1	History of machine learning.....	19
3.2	Machine learning models.....	20
3.2.1	Supervised learning.....	21
3.2.2	Unsupervised learning.....	22
3.2.3	Reinforcement learning.....	24
3.3	Machine learning algorithms.....	26
3.3.1	Random forest.....	26
3.3.2	Extreme gradient boosting (XGB).....	28
3.3.3	Adaptive boosting (AdaBoost).....	29
3.3.4	Gradient boosting.....	30
3.3.5	K-nearest neighbours (KNN).....	30
CHAPTER 4: METHODOLOGY.....		33
4.1	Data collection (Database preparation).....	33
4.1.1	Descriptive statistics.....	35
4.1.2	Data exploration.....	37
4.2	Data preprocessing.....	42
4.3	Features selection.....	44
CHAPTER 5: RESULTS AND DISCUSSION.....		45
5.1	Metrics of performance.....	45
5.2	Cross-validation.....	46
5.3	Performance of models.....	47
5.4	Feature importance analysis.....	51

CHAPTER 6: CONCLUSION	59
6.1 Summary	59
6.2 Future work and recommendation	60
REFERENCE	62
LIST OF PUBLICATIONS AND PAPERS PRESENTED	67
APPENDICES	69

University of Malaya

LIST OF FIGURES

Figure 2.1:	Energy level diagram of typical OLED device with doped emitting layer.....	6
Figure 2.2:	Spin coating process. From left: solution is dropped onto substrate, substrate is spun at several hundred to thousand RPM, solution is left to dry.....	7
Figure 2.3:	Typical OLED structures consisting different layers with a specific functions.....	8
Figure 2.4:	Example of phosphorescent emitters. Ir(ppy) ₃ , left and FIrpic, right	11
Figure 2.5:	Weighted luminosity functions. Green (photopic) represents human eyes sensitivity in bright conditions, black (scotopic) in low lights	16
Figure 2.6:	CIE coordinates	17
Figure 3.1:	Example of supervised learning: Classification and Regression.....	21
Figure 3.2:	PCA used in visualizing 64-dimensional data in two dimensions	23
Figure 3.3:	t-SNE used in visualizing 64-dimensional data in two dimensions	23
Figure 3.4:	Concept used in reinforcement learning where reward is given when the answer given is correct	24
Figure 3.5:	Example of decision tree used to classify Iris flowers based on their petal length and width.....	27
Figure 3.6:	Nearest neighbours for classification, where K=3. The closest three neighbours decide the class of unlabelled instance.....	31
Figure 4.1:	Correlation between the features used in the modelling. The heatmap is broken down in to four parts for better visualization.....	39
Figure 4.2:	Technique used to deal with device with different number of layers	43
Figure 5.1:	Examples of a) underfitting, b) nice fitting and c) overfitting	46
Figure 5.2:	Cross validation example using k-fold, where k = 5. The testing and training data are changed for every experiment	47

Figure 5.3:	Plot of predicted device efficiency versus true experimental efficiency using random forest regression algorithm. The true efficiency is the current efficiency of devices measured at 1000 cdm^{-2} . X-axis is the predicted efficiency and y-axis is the true experimental value.	49
Figure 5.4:	Feature importance based on the random forest algorithm.	52
Figure 5.5:	Boxplot comparison of data distribution between triplet energy of host material and dopant.....	53
Figure 5.6:	Current efficiency of generated blue PhOLED devices with various host triplet energy. Blue line shows the triplet energy for FIrpic	54
Figure 5.7:	Contour plot a) – c) shows the relation between triplet energy of HTL and ETL with device efficiency. EML triplet energy is fixed at 2.60, 2.80, 3.00 eV respectively. Contour plot d) –f) shows relation between HOMO level of HTL and ETL with device efficiency. HOMO level for the host material is fixed at 5.60, 5.80 and 6.0 eV respectively	56
Figure 5.8:	Relation between thicknesses of ETL, HTL with the device efficiency. EML thickness increases by 5 nm from a) 10 nm to f) 35 nm.....	58

LIST OF TABLES

Table 4.1:	Features along with its meaning used for modelling and the linear correlation with respect to device efficiency.....	34
Table 4.2:	Descriptive statistics and distribution of features collected from literature.....	36
Table 5.1:	Performance of different machine learning models on cross validated training data and test set. Bold shows the best result.	48
Table 5.2:	Performance of different machine learning models on different training sizes.....	50

University of Malaysia

LIST OF SYMBOLS AND ABBREVIATIONS

AdaBoost	: Adaptive boosting
AI	: Artificial intelligence
Al	: Aluminium
Alq ₃	: Tris(8-hydroxyquinolato)aluminium
BOBP	: 2,2'-bis(5-phenyl-1,3,4-oxadiazol-2-yl)biphenyl
Ca	: Calcium
CART	: Classification and regression tree
CBP	: 4,4'-Bis(N-carbazolyl)-1,1'-biphenyl
CIE	: <i>Commision International de l'Eclairage chromaticity</i>
Cs ₂ CO ₃	: Caesium carbonate
CsF	: Caesium fluoride
EIL	: Electron injection layer
EML	: Emitting layer
EQE	: External quantum efficiency
ETL	: Electron transport layer
GBRT	: Gradient Boosted Regression Trees
GPU	: Graphic processing unit
HIL	: Hole injection layer
HOMO	: Highest occupied molecular orbital
HTL	: Hole transport layer
IQE	: Internal quantum efficiency
Ir	: Iridium
ISC	: Intersystem crossing
ITO	: Indium tin oxide

KNN	: K-nearest neighbours
LCD	: Liquid crystal display
LiF	: Lithium fluoride
Liq	: 8-Hydroxyquinolinolato-lithium
LUMO	: Lowest unoccupied molecular orbital
MAE	: Mean absolute error
Mg	: Magnesium
ML	: Machine learning
MNIST database	: Modified National Institute of Standards and Technology database
OLED	: Organic light-emitting diode
PCA	: Principal component analysis
PEDOT:PSS	: Poly(3,4-ethylenedioxythiophene):poly(styrene sulfonate)
PhOLED	: Phosphorescent organic light-emitting diode
Pt	: Platinum
PVK	: Poly(9-vinylcarbazole)
RMSE	: Root mean squared error
TADF	: Thermally activated delayed fluorescent
TCTA	: 4,4',4''-tris(N-carbazolyl)triphenylamine
TDATA	: 4,40,400-tris(N-diphenyl-amino)triphenylamine
TPBI	: 2,2',2''-(1,3,5-Benzinetriyl)-tris(1-phenyl-1-H-benzimidazole)
TPU	: Tensor processing unit
t-SNE	: t-distributed Stochastic Neighbour Embedding
UV	: Ultraviolet
XGB	: Extreme gradient boosting
ZnO	: Zinc oxide

LIST OF APPENDICES

Appendix A: Python programming code used for this work.....	69
Appendix B: Sample of data used for this work.....	72

University of Malaya

CHAPTER 1: INTRODUCTION

1.1 Introduction

Organic light-emitting diode (OLED) is steadily transitioning into display market, replacing the traditional liquid crystal display (LCD). This transition is caused by the interesting advantages OLED has over LCD, such as high contrast and refresh rate, glare free, light weight, wide viewing angle and can be made very thin. The thickness of light emitting layer in OLED is only few nanometres thick and depending on the substrate used, it can even be made flexible (Lee et al., 2014; Park et al., 2011). In addition, OLED emits its own light, thus it does not need a backlight source that is crucial in LCD screen. Without a backlight source, each OLED pixel can emit its own light which is fundamentally different than LCD. This means OLED pixel can save energy consumption and produce true black when it is turned off, something LCD cannot do with the backlight on even with great dimming technology.

This advantages of OLED are made possible by the tremendous amount of research done on this particular subject. Currently, research on OLED is still huge with researchers aiming to fix some of the problems with OLED, namely its cost, stability and efficiency. OLED is expensive mainly because of two reasons, its material (Im et al., 2017) and production cost (Xu et al., 2014). These problems will be explained further in the next chapter, and how this research can provide another perspective on this matter.

1.2 Problem statement

OLED offers many advantages and shows immense potential to be the dominant display technology in near future. However, with great features, comes few drawbacks. High price point of OLED screen at the moment is limiting its application for high-end, flagship and premium devices only. The source of this problem is that some OLED

incorporated rare and expensive earth metals in its light emitting layer such as Platinum (Pt) and Iridium (Ir) to increase efficiency (Im et al., 2017). Moreover, most materials are also deposited using high vacuum deposition process which is very costly. The number of OLED related publication is growing exponentially year by year, in hope to tackle the problems faced by OLED.

1.3 Motivation and objectives

Efficiency is one of the main drawbacks for OLEDs to be used for practical application. Fabricating highly efficient devices is no easy task because modern OLED architectures and structures are a bit more complex than what it used to be. The new OLED structure has multiple layers, each layer has distinct properties and functionality. Investigating new materials for a particular layer experimentally is very time consuming because the compatibility of the materials with neighbouring layer needs to be considered. This is especially true for solution processed OLED. What's more, the problem multiplies with each additional number of layers in a device.

To solve this problem, this research work is trying to use a different approach. This is where machine learning comes into play. Combining statistical analysis with some matrix computation and mathematical algorithms, it can see a bigger picture of what contributes to its efficiency. Thanks to the attention that OLED has drawn, huge number of researchers are rapidly finding solutions to improve OLED devices, and this is proven by the number of papers published every year. This helps the analysis since machine learning algorithms requires a lot of data to work.

The objectives of this research are:

- To investigate the efficacy of machine learning and statistical analysis to find out relationship between OLED efficiency and materials parameters

- To predict device efficiency using the description of each material
- To find out crucial factor impacting efficiency of OLED device

The results from the research can be useful for synthetic chemist and device engineer to fabricate extremely efficient device.

1.4 Outline for dissertation

Chapter one provides research background of OLED and introduction of techniques that will be used for this study. This chapter also addresses some problems with OLED in general and my motivation to do this research. Chapter two brings in the depth of background information of working principle of OLED device, specifically blue phosphorescent OLED (PhOLED). The current problems and limitations of current devices and experimental methods are also explained. To bring audiences into a bigger picture of the device efficiency problem, a section detailing how the metrics are calculated is also included.

In chapter three, a short history of machine learning and artificial intelligence are included to illustrate how this area of research became what it is as of today. Types of machine learning models are briefly discussed, to give an idea of what kind of machine learning is being used in today's technologies. Next, all machine learning algorithms used in this research are discussed in terms of the advantages and disadvantages of each algorithm.

Chapter four details the data collection and preparation processes which includes data exploration, features selection and data pre-processing. In chapter five, the results of the machine learning based models are discussed. A further analysis is also explained on how each feature is represented in the built algorithms. Model performance is also included based on the specified metrics.

Last but not least, chapter six concludes this dissertation with a summary of the experiment and work done. This chapter also provides insight for future work alongside some great recommendations to move forward with this type of research.

University of Malaya

CHAPTER 2: LITERATURE REVIEW

2.1 Organic Light-Emitting Diode (OLED)

Organic light-emitting diode (OLED) is a semiconducting device in which emits light upon application of electricity. The simplest structure of an OLED is an emitting layer consisting of organic material, sandwiched between anode and metal cathode. Figure 2.1 shows an example of typical OLED layers in energy level diagram. When electricity is applied through the anode and cathode, light is produced as a result from the combination of positive and negative charges from respective electrodes. If the resultant exciton is singlet, the process is called fluorescence, in which light produced (photon emission) is from relaxation singlet excitons from excited state (Lakowicz, 2013). Traditional OLED devices make use of this principle to produce light from the organic materials. A problem with early OLED devices was that they required high voltage in order to operate, from 30V up to several hundred volt (Bernanose, 1955; Vincett et al., 1982), which rendered them impractical for real life applications. It was not until 1987, when Tang and Van Slyke first fabricated device that reaches brightness over 1000 cd/m² while maintaining low driving voltage (Tang & Vanslyke, 1987). This achievement had a huge impact and attracted more researchers to study about OLED and eventually, led to the implementation of OLED in today's display technology.

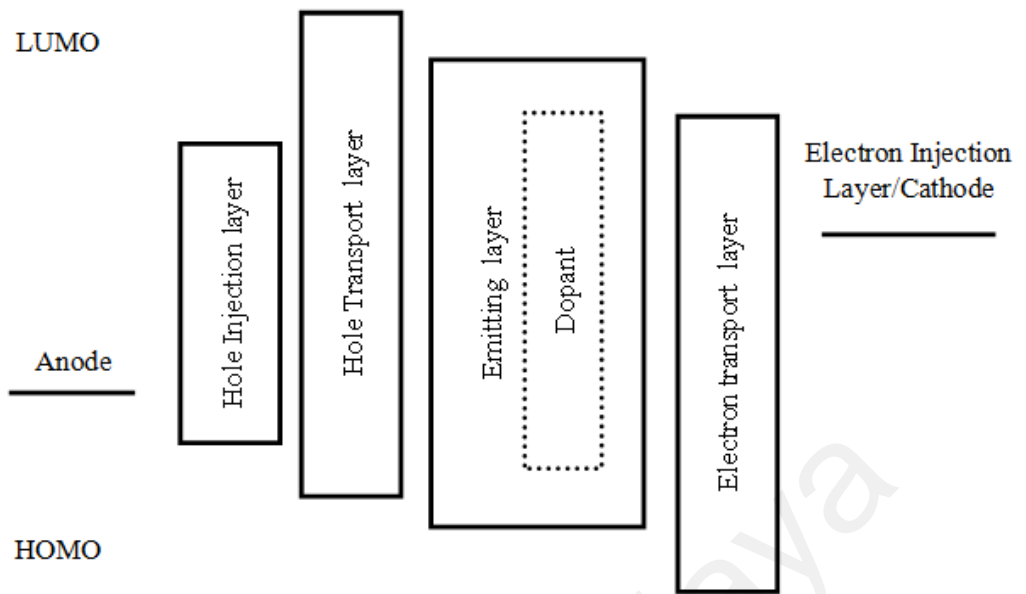


Figure 2.1: Energy level diagram of typical OLED device with doped emitting layer.

Generally, OLED materials are from two family types, small molecules and polymers. Small molecule materials, such as tris(8-hydroxyquinolino)aluminium (Alq_3), are usually deposited through vacuum deposition process. Polymer materials on the other hand, have high molecular weight. One example of polymer material is poly(9-vinylcarbazole) (PVK), which is widely used in device fabrication, but it is not suitable for vacuum deposition. Solution processing is more suitable for polymer materials as they tend to have good solubility and good film formation (Granström & Inganäs, 1996). Some commonly used solution processing techniques include spin coating, as illustrated in Figure 2.2, inkjet printing and doctor blade. These techniques are more suitable for large area printing and also significantly cheaper compared to vacuum deposition process. However, it is more difficult to fabricate multilayer device using solution process since lots of things need to be considered. For instance, solubility of materials needed to be considered to avoid being washed out when subsequent layer is deposited.



Figure 2.2: Spin coating process. From left: solution is dropped onto substrate, substrate is spun at several hundred to thousand RPM, solution is left to dry.

Phosphorescent light-emitting diode (PhOLED), a newer generation of OLED, made its first appearance in 1998, by Baldo *et al.* (Baldo et al., 1998). One major difference between fluorescence and phosphorescence devices is the presence of phosphorescence dye in the later devices, typically from heavy metal compound such as Iridium (Ir) and Platinum (Pt) molecules replacing the fluorescence emitter in the former device (Im et al., 2017). With the dye (which is also called guest molecule) present, PhOLED devices are able to harvest both singlet and triplet excitons instead of just singlet in fluorescent OLED (Im et al., 2017). This is a huge step in OLED development since triplet excitons made up 75% of the excitons produced. Harvesting triplet excitons enable devices to theoretically achieve 100% internal quantum efficiency (IQE) in theory.

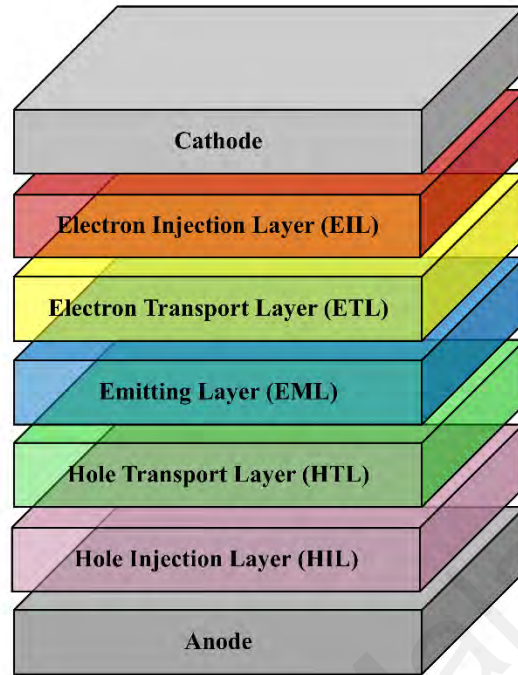


Figure 2.3: Typical OLED structures consisting different layers with a specific functions.

Figure 2.3 shows the device configuration of a typical PhOLED device in which the organic materials are sandwiched between the cathode and anode that inject electrons and holes respectively into the device. One big advantage of this multilayer, sandwich configuration is that it can confine the charges and excitons inside the emitting layer. This is done by placing charge transport layers adjacent to the emitting layer, which also sometimes serves as charge blocking layer (Yin et al., 2016). The emitting layer of OLED usually consists fluorescent emitter or a mix of host and phosphorescence dye materials for PhOLED. The cathode is usually made from reflective materials such as Aluminium (Al) to reflect the light back and out of the device through the anode. For this purpose, it is important for anode to be transparent so that maximum light intensity can be emitted. A widely used anode for OLED is Indium tin oxide (ITO), which is highly transparent and has high work function to promote hole injection.

Organic materials are well-known to be highly sensitive to water, oxygen and ultraviolet light. Thus, encapsulation technique is used to protect the materials, increasing lifetime. Ultraviolet (UV) curable epoxy is used alongside with glass lid to protect the organic materials from degradation. The effectiveness of encapsulation is also one of the major contributors to OLED stability and long lifetime.

2.2 Working principles and parameters of OLED

When a voltage is applied between two electrodes, the cathode pumps electrons into the dye-containing emission layer located between the two electrodes while the anode supplies holes. These holes can jump to the emission layer and recombine with the electron to form bound electron–hole pairs, the excitons. The return of the excitons to the ground state, i.e. the recombination of holes and electrons, leads to a relaxation of the energy levels of the electrons in the form of light (photon) (Lakowicz, 2013). The design of sandwiched layers facilitates charge injection and enhances the recombination rate of electrons and holes (Xu et al., 2014).

To get a clearer picture of the working principle of an OLED device, it is necessary to take a look at each layer individually, in terms of its use case and functionality. Next subsections will go through the common materials used for each layer, the criteria and requirements needed for high current efficiencies. Also included, are some prior research done to improve these layers and device performance.

2.2.1 Emitting layer

Emitting layer (EML) is the layer responsible for all lights coming out of the device, thus can be considered the most important part of an OLED device. In fact, early devices had only one organic material as emitting layer sandwiched between anode and cathode (Vincett et al., 1982). The organic materials used for the emitting layer determines the

colour that comes out from the OLED devices. In general, emission wavelength is controlled by the bandgap of the EML material, as well as the device structure (Wei et al., 2010).

EML is the area in which carrier recombination occurs as recombination in another layer would not result in maximum light emission, or no emission at all, thus reducing the efficiency. Moreover, exciton formation in outside of emitting layer will affect the light emission, inducing colour impurity. Recently, OLED devices are taking advantage of doped EML for increased efficiency (Zhu & Yang, 2013), and this is particularly true for PhOLED. Doped devices employed host materials in the EML to combat triplet-triplet annihilation of the dopant emitter (Tao et al., 2011). There are several types of host materials such as hole-transport host materials (4,4',4''-tris(N-carbazolyl)triphenylamine, TCTA and 4,4'-Bis(N-carbazolyl)-1,1'-biphenyl, CBP), electron-transport host materials (2,2'-bis(5-phenyl-1,3,4-oxadiazol-2-yl)biphenyl, TPBI and 2,2',2''-(1,3,5-Benzinetriyl)-tris(1-phenyl-1-H-benzimidazole), BOBPs) (Leung et al., 2007) and bipolar transport host materials (carbazole, Cz/ oxadiazole, OXD hybrid) (Tao et al., 2011). Each of these type serves to facilitate charge movements into the EML and to achieve balance of both electron and hole in EML, which is crucial for exciton formation.

For host material to be efficient, it must provide an excellent energy transfer to the dopant materials. The other requirement is that it must have a wide band gap and a higher triplet energy than the guest. High triplet energy prevents energy transfer from guest back to host and also confines triplet excitons in emitting layer (Tokito et al., 2003; Woon et al., 2015). Matching HOMO and LUMO level with neighbouring layers throughout the device is also critical in reducing driving voltage of the device by lowering the charge injection barrier. Furthermore, device lifetime can be prolonged by using host materials with good morphological and thermal stability (Zhu & Yang, 2013).

Another component of emitting materials for PhOLED is the phosphorescent dye or the guest emitter. Numerous phosphorescent emitters have been developed since its introduction because of their high efficiency. These emitters make use of heavy metal complexes such as Iridium and platinum. Some common dopant emitters with Iridium complexes are FIrpic, Ir(ppy)₃ and (piq)₂Ir(acac) for blue, green and red PhOLED respectively. Figure 2.4 shows some example of widely used, Iridium based phosphorescent emitter.



Figure 2.4: Example of phosphorescent emitters. Ir(ppy)₃, left and FIrpic, right.

In general, blue Ir based emitters can be classified into three groups, arylpyridine-, imidazole- and carbene-type compounds (Im et al., 2017). For example, imidazole-type emitter has a better lifetime than the other type of emitters. This is due to the weak electron deficiency in the imidazole unit, lowering the LUMO level, increasing the HOMO-LUMO gap and thus inducing blue shift in the wavelength emitted. The downside of this type of emitter is that the colour purity is poor such that it can only produce colour in the sky blue region which is not enough for full colour display.

2.2.2 Anode and injection/buffer layer

The most commonly used anode material is Indium Tin Oxide (ITO) prepared on glass substrate. ITO has several features that make it desirable as an anode. First, ITO is a transparent material, which is the most important criteria since light must go through this

layer for bottom emitting OLED. Second, it has a high work function, typically around 4.5 eV, which can be further increased when treated with oxygen plasma. Plasma treatment is also shown to enhance device performance, lower driving voltage and increase device lifetime (Wu et al., 1997).

Another layer called buffer layer (sometimes called hole injection layer) is often added in between the anode and the hole transport layer to boost device performance. This layer works by decreasing the energy barrier between HOMO level of hole transport layer and ITO. Some commonly used materials include Poly(3,4-ethylenedioxythiophene):poly(styrene sulfonate) (PEDOT:PSS) and 4,4',4''-tris(N-diphenyl-amino)triphenylamine (TDATA) (Wang et al., 2008).

PEDOT:PSS is a very good hole injection layer because of its good film-forming properties, high conductivity and visibility. The performance of devices incorporating PEDOT:PSS as injection layer can be further improved by mixing it with inorganic particles such as metal nanoparticles (gold, zinc, silver, carbon). Insertion of these materials improve electrical properties and at the same time does not reduce the performance in terms of optical properties (Choulis et al., 2006).

2.2.3 Cathode and injection/buffer layer

Low to medium range of work function metals such as Calcium (Ca), Aluminium (Al) and Magnesium (Mg) are the most commonly used materials for cathode. The reason is that cathode has to be excellent in electron injection, making these electronegative metal a natural choice (Scott & Malliaras, 1999).

It was also observed that fermi level pinning often occurs at the metal-organic layer interface. In order to prevent this problem, an ultrathin layer of insulator materials like caesium fluoride (CsF) and lithium fluoride (LiF) often inserted in between the two

layers. The fluorides from these materials prevent chemical bonding of Al to the organic materials. Furthermore, this buffer layer helps the formation of dipole charge layer, which increases the effective work function of metal cathode, hence reducing the barrier gap for electron injection (Shinar & Savvateev, 2004). The presence of this buffer layers also allows the voltage to drop across it, moving the Fermi level of Al to be aligned with the adjacent transport layer (Jabbour et al., 1997).

2.2.4 Transport layer

The transport layer serves multiple purposes in an OLED device. First, it lowers the energy barriers between the electrodes and the emitting layer (Zhou et al., 2006). This is important as most emitting layers does not have matching HOMO and LUMO level with the respective electrodes for efficient charge injection, causing high energy barrier. Second, transport layers move the carrier recombination area well away from the organic-metal electrode interface. As the recombination concentrates on the HTL/ETL – EML interfaces, exciton quenching caused by dissociation at the electrodes can be greatly reduced (Scott & Malliaras, 1999). Additional transport layers are also added to prevent abrupt changes of the energy barrier at the metal-organic interface, which can cause huge mismatch for the HOMO and LUMO levels.

To achieve device with superior performance, there are several requirements for electron and hole transport layers. Hole transport layer (HTL), commonly contains electron donating moieties for good hole mobility. In addition, HTL must have suitable HOMO level to lower hole injection barrier from anode to the emitting layer and at the same time suitable LUMO level to block electron from exiting the emitting layer. For exciton confinement, high triplet energy is also desired in HTL materials (Tao et al., 2011). Some commonly used HTL are TCTA (E_T : 2.76 eV) and CBP (E_T : 2.56 eV) (Shirota & Kageyama, 2007)

Electron transport layer (ETL) on the other hand, is the opposite. ETL often contains electron withdrawing group in their structures. Efficient ETL has to have good electron mobility to transport electron injected from cathode to EML. Appropriate HOMO and LUMO level are needed to block holes from being injected into EML and to ease electron injection. Additional requirements include high triplet energy and high thermal stability for efficient exciton confinement and longer device lifetime (Tao et al., 2011). Alq₃ (E_T : 2.0 eV) (Baldo et al., 1998; Tang & Vanslyke, 1987) and TPBI (E_T : 2.74 eV) are some of the common ETL materials.

2.3 Phosphorescent Organic Light-Emitting Diode (PhOLED)

Phosphorescent Organic Light-Emitting Diode (PhOLED) is another type of OLED. The phosphorescent emitters often acted as guests inside a host. The major difference of PhOLED compared to OLED is the type of exciton harvested when excited electrically. Generally, exciton from charge injection will have a ratio singlet: triplet of 1: 3 (Helfrich & Schneider, 1965). Fluorescent OLED emits light when singlet excitons transition from excited state to ground state. In this conventional method, triplet excitons went through this transition non-radiatively (Im et al., 2017) and hence they are often called dark states. The presence of Platinum (Pt) or Iridium (Ir) as a complex in a emitter lift the non-radiative transition of the triplet states (Im et al., 2017). The singlet excitons formed in PhOLED are converted to triplet excitons by intersystem crossing, therefore all excitons can produce radiation by phosphorescence. One major advantage of this process is that the device is now theoretically possible of achieving 100% internal quantum efficiency (IQE) (Im et al., 2017). This is a huge improvement from 25% maximum IQE from fluorescent devices that harvest singlet exciton alone.

Light emission in phosphorescent doped devices can be achieved in three ways (Tao et al., 2011). First is when the charges are trapped and excitons are formed in the host

material, and consequently, energy is transferred to the triplet emitter. Initially, only singlet excitons are formed upon electrical excitation. The transfer of the exciton from host to phosphor guest are done via Förster (long range) and Dexter (short-range) energy transfer. Consequently, the excitons are converted to triplet excitons by intersystem crossing (ISC). Second, triplet excitons can also be formed directly inside the host material, which then transferred to the dopant via Dexter energy transfer. Light emission is observed when the triplet excitons decay radiatively. Third is that the triplet emitter itself trapped the charges, thus forcing the recombination to occur on this molecule generating triplet excitons (Yersin, 2008).

Confinement of exciton in EML is important in both fluorescent and phosphorescent OLEDs. In addition, since the triplet exciton has a longer diffusion length, it became more important to deploy device configuration that focuses on exciton confinement (Djurovich & Thompson, 2007). If triplet exciton produced is not restricted to the EML, it can diffuse to other neighbouring layers, causing reduced efficiency and broader emission spectrum.

2.4 Device efficiency

Since the main goal of this thesis is to predict and increase the efficiency of PhOLED devices, it is important to discuss how this metric is measured. There are several different ways of how device efficiency are calculated (Forrest et al., 2003). One way is to calculate the brightness of the light emitted from the devices. The brightness of produced light in visible spectrum (~400 – 700nm) is measured in candela, cd, the SI unit for luminous intensity. This unit, however, is biased towards the human sensitivity towards light, and peaked around 555nm (green region) as shown in Figure 2.5. Therefore, when lights of different spectrum (different colour) are measured, the candela measurement is going to favour green coloured spectrum heavily even though they emit the same power.

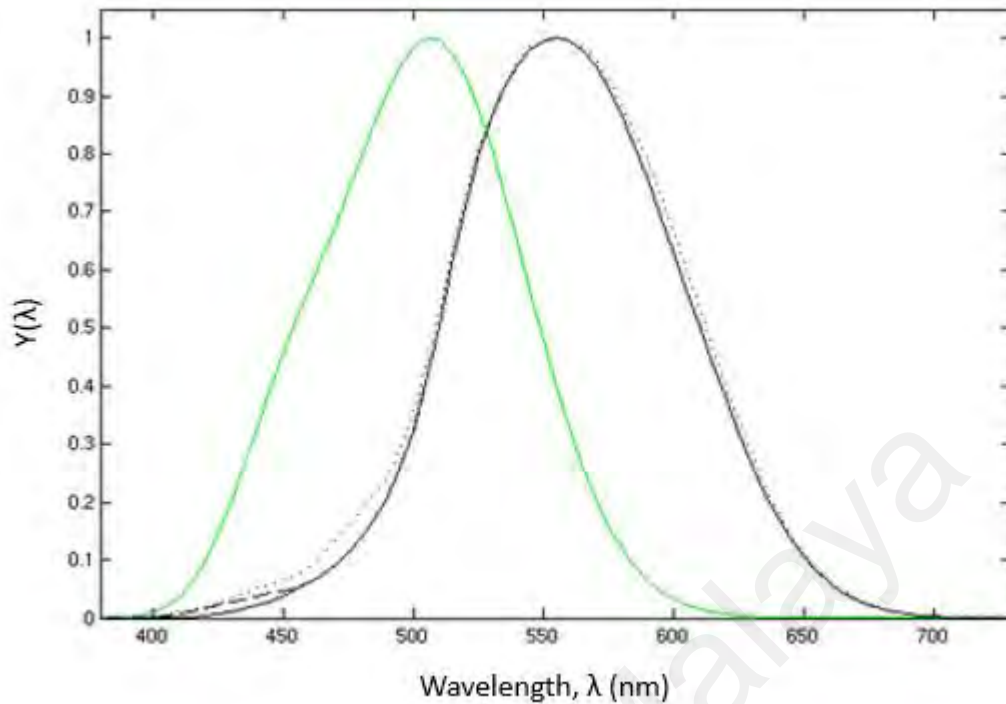


Figure 2.5: Weighted luminosity functions. Green (photopic) represents human eyes sensitivity in bright conditions, black (scotopic) in low lights.

Two main brightness measurements that are being used for OLED devices are candela per area (cd/m^2) and lumen per power (lm/W), also known as current efficiency and power efficiency respectively. For brightness, which is also known as nit, the light emission is assumed to be Lambertian. This metric is useful to quantify the brightness for display applications. Power efficiency on the other hand, measures the ratio of luminous power emitted to the total electrical power at a certain voltage.

These two measurements however, do not do justice to light with different emission spectra since they factor in human eye sensitivity. So another form of metric commonly used is external quantum efficiency (EQE), which basically measures the ratio of the number photons emitted in the viewing direction per number of electron injected.

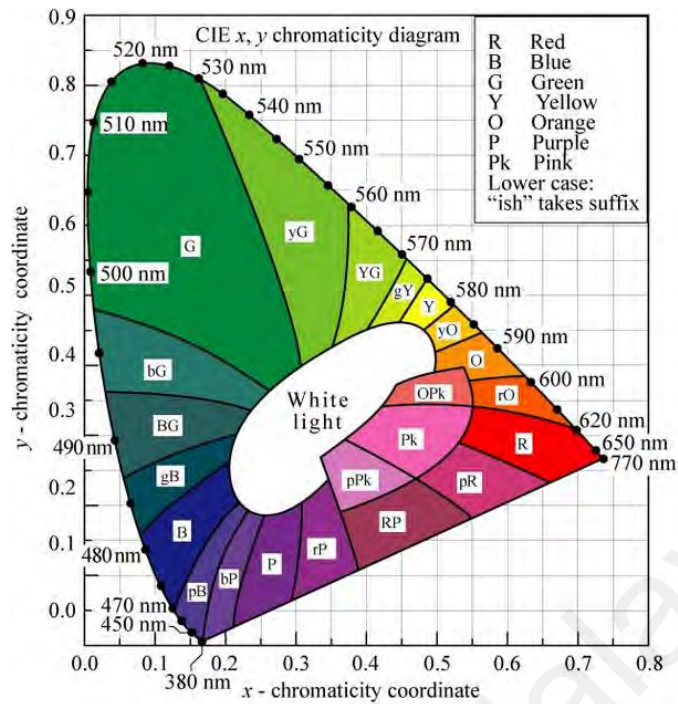


Figure 2.6: CIE coordinates.

Another important thing about emitted light is the width of the emission spectrum and its Commission International de l'Eclairage chromaticity (CIE) coordinates, as shown in Figure 2.6. These two measurements do not measure the efficiency of the device but rather its colour shades. For instance, OLED device emitting blue colour generally has x-coordinate between $[0 - 0.3]$ and y-coordinate between $[0 - 0.4]$. However, for full display application, deep blue emission is required (y-coordinate < 0.15) so that the colour gamut for the entire device can be wider, and more colours can be produced.

2.5 Blue PhOLED limitations

PhOLEDs at the moment, has a relatively high efficiency among other OLED technologies like fluorescence and thermally activated delayed fluorescence (TADF). However, the efficiency is still regarded as low when compared to another lighting technology like LED for general lighting and display purposes. The main culprit for this low efficiency and stability of a full colour PhOLED device is the blue emitter, which has way lower efficiency and stability than its other colours counterpart. For this exact reason,

some devices are using the fluorescent emitter for the blue-producing part, combined with red and green phosphorescence in order to achieve full colour display (Schwartz et al., 2009). This technique is also quite useful in addressing the low stability and longevity of blue PhOLED emitters, which originated from the low endurance of blue materials to the high energy emission of blue light (Song & Lee, 2017).

Blue emitting devices need to fulfil certain criteria to achieve high efficiency. For example, blue devices require host with high triplet energy. The choice of host material for another emitter, red and green, is relatively easier because of their low triplet energy. Furthermore, for blue emitting materials, both fluorescent and phosphorescent emitters have intrinsic wide bandgap, complicating the charge injection process (Zhu & Yang, 2013). There are quite a number of approaches done to increase the efficiency of blue devices, and the main approaches can be categorized into three; (i) increasing LUMO or lowering HOMO in order to widen energy gap; (ii) introducing ancillary ligands with strong field effects; and (iii) shortening the effective conjugation length of molecules (Xu et al., 2014).

Data from hundreds of blue PhOLED devices was collected to be analysed in this study to see which of the criterion in a device contributes the most to the efficiency, based on statistical models.

CHAPTER 3: MACHINE LEARNING

3.1 History of machine learning

Before this chapter dives straight into how machine learning is used for this research, it is better to provide a brief introduction about machine learning and artificial intelligence (AI). Simply put, machine learning processes input data and map it into output which is either a class (nominal) or continuous value. There are several type of machine learning models and they will be discussed individually in the next section.

One of the earliest line fitting technique, the least square method is the basis of some machine learning algorithms like linear regression and logistic regression to name a few. Since then, lots of new techniques have been developed such as Bayes theorem, Markov chains and neural network which invoked further interest in the field. The area of machine learning and artificial intelligence were booming since then with lots of institutions and government agencies funding the research. This created a hype of what machine learning and artificial intelligence can achieve in real life application.

After some times, in the 70s, the artificial intelligence achievements and discoveries met a plateau. Very little progress is observed in the fields, causing pessimism about the effectiveness of machine learning and its real world's contribution. Consequently, funding for research was cut by the US and British government, causing a downtime period for the field which is later known as "AI winter". Research on AI then changed since AI had become a dirty word and was to be avoided. The term AI was rebranded to other terms like search algorithms, intelligent programs and many more.

In the 1980s, AI was revived because of multiple reasons. First was the increased in computing power. Computers has become more powerful so that more complex operations and calculations can be done faster compared to the previous generations.

Second, the field now focused more on solving specific problems rather than vague abstract philosophical questions and problems. AI also became more connected to other fields such as mathematics and statistics, which allowed the field to mature and follow the standard set by the fields. Third, backpropagation was rediscovered in this period which is of huge importance to the machine learning algorithms especially the artificial neural network.

Recently, machine learning and artificial intelligence became a hot topic once again. This resurgence is caused mainly by two factors, i) plenty of data, especially labelled data, and ii) high computation power to process them. Using graphic processing unit (GPU) and tensor processing unit (TPU), heavily invested by Google, have accelerated the machine learning research. These new technologies are proven to be much faster for machine learning computation than those regular processors. Cloud computing also allows researchers and industries to gain access to powerful computer easily without having to deal with the hassle of setting up local servers and such.

Nowadays, machine learning and AI are everywhere and people sometimes take it for granted. AI is in smartphones doing tasks like autocorrect and autocomplete when typing an email, smart personal assistant such as Siri, Alexa and Google assistant help people in variety of tasks from setting an appointment to making phone calls. Autonomous car has been built with smart sensors and algorithms, is said to be capable of minimizing car accident rates by reducing errors caused by human.

3.2 Machine learning models

Now that the chapter has discussed briefly about history of machine learning, let's take a look at the models or algorithms and also different type of machine learning. Machine

learning models are divided into three main categories namely supervised learning, unsupervised learning and reinforcement learning.

3.2.1 Supervised learning

Generally speaking, supervised learning can only be used with target variable present and the target is labelled. Common supervised learning algorithms include linear regression, naïve Bayes, support vector machine, decision trees and logistic regression. Supervised learning is used for two types of problems: classification and regression.

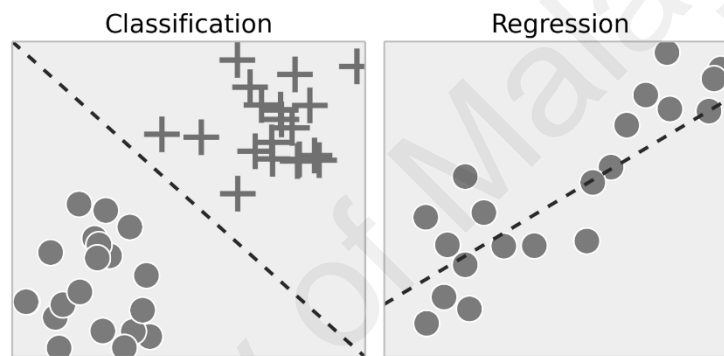


Figure 3.1: Example of supervised learning: Classification and regression.

For classification problem, the algorithm is trying to learn based on the data (features) given to it and produce a prediction for unseen data. For instance, in Figure 3.1 above, the classifier is trying to classify the circles from the plus signs, based on their 2-d coordinates. Then, for any given point on the coordinate, the model will make a prediction whether the symbol is a plus or circle. The same process can be repeated for regression process, but instead of predicting a discrete class, the model will predict a continuous value (VanderPlas, 2016). The example given above is, of course, a very simple instance with only two variables (the x and y coordinates). One might say that machine learning is not needed for such task since human can easily classify them. But imagine the same classification problem, but with hundreds of parameters instead of just two, and some of the variables are non-linear, to make things worse. This is when human intuition often

times fails, processing high dimensional problems (Domingos, 2012). Machine on the other hand, can handle multidimensional problems well, given enough resources and data points.

Some use cases of supervised learning is spam detection, image and pattern recognition. Supervised learning is the most popular type of learning, among the three mentioned earlier, but this type of learning requires a lot of labelled data, which is very scarce. For this very reason, unsupervised learning or semi-supervised is preferred and even said to be the future of artificial intelligence.

3.2.2 Unsupervised learning

Unsupervised learning has no need for labelled data and generally used for clustering purposes. K-means and the nearest neighbours are well known algorithms for this class. Another use case for unsupervised learning is to find the structure of the data.

Dimensionality reduction is one of the great use of unsupervised learning. Algorithms such as principal component analysis (PCA) and t-distributed Stochastic Neighbour Embedding (t-SNE) (Maaten & Hinton, 2008) are primarily used for dimensionality reduction. Moreover, these techniques are also used for visualization, feature engineering, noise filtering and many more. A common example for PCA and t-SNE use case is the visualization of Modified National Institute of Standards and Technology database (MNIST) handwritten digit dataset. In this example, the dimension of images of handwritten digit, from zero to nine, is being reduced from 64 dimensions to just two dimensions for visualization. Figure 3.2 and Figure 3.3 show example of how PCA and t-SNE work respectively.

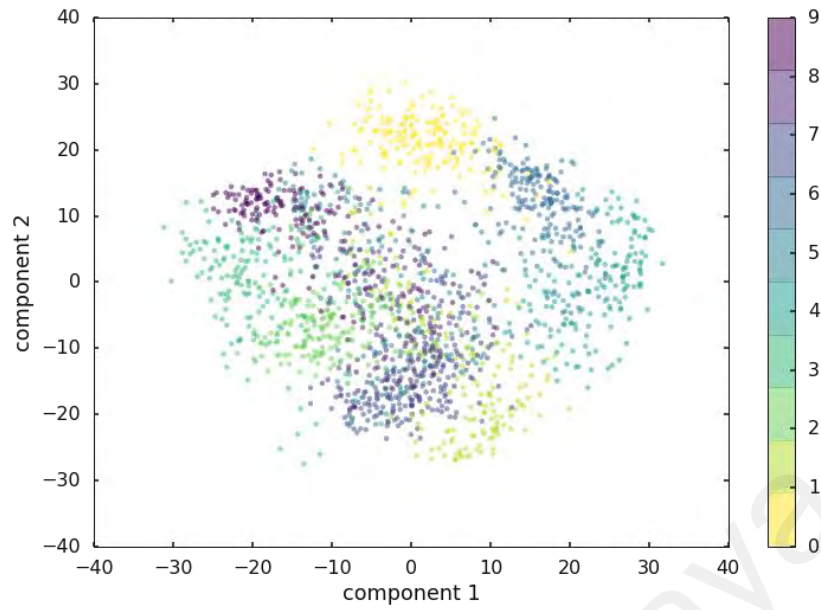


Figure 3.2: PCA used in visualizing 64-dimensional data in two dimensions.

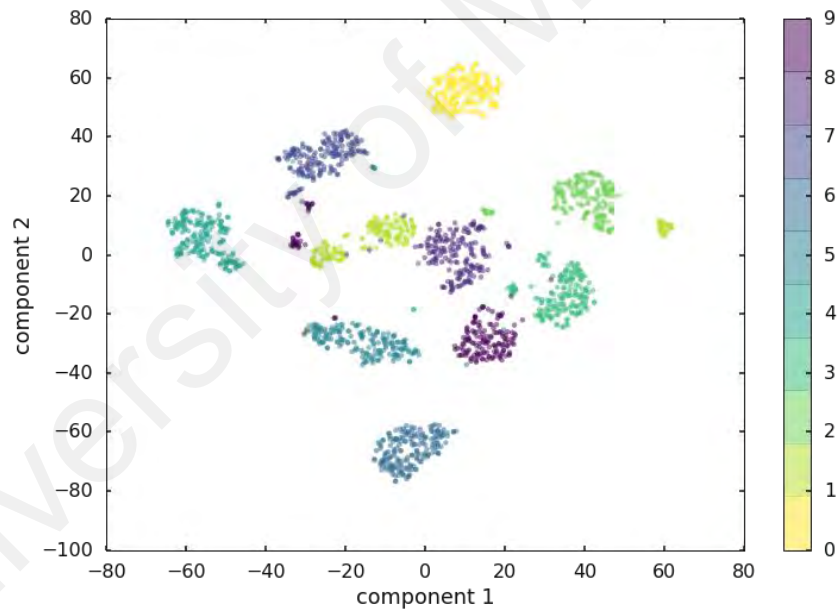


Figure 3.3: t-SNE used in visualizing 64-dimensional data in two dimensions.

From the figures above, it can be seen that images of handwritten digits are reduced to two dimensions, and the data points are clustered automatically without implicitly using the label. This process is done entirely based on the images, and the clusters are formed based on image similarity alone.

3.2.3 Reinforcement learning

Like supervised learning, reinforcement learning maps the output from the input. The difference between both methods is that supervised learning has a true output (discrete class for classification and continuous values for regression), in which the error can be calculated. On the other hand, reinforcement learning process usually provides some kind of reward and punishment system to achieve a goal. The algorithm will try to achieve the goal by maximizing the reward and minimizing the punishment.

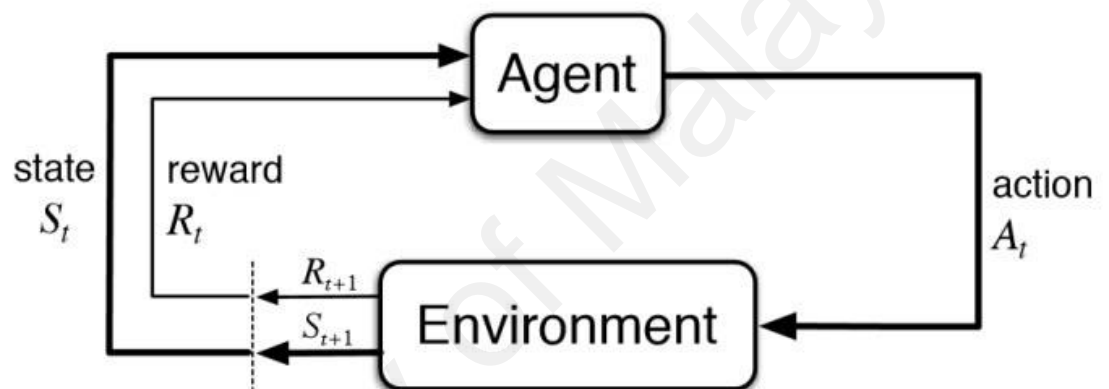


Figure 3.4: Concept used in reinforcement learning where reward is given when the answer given is correct.

Figure 3.4 describes the key concept of reinforcement learning. The agent takes action based on the observations received from the environment, which come in terms of reward and state. Based on action taken, the reward will inform the agent whether the action was good or not, and the environment will output the next state.

Reinforcement learning techniques are used in robotics and also for beating board games and video games. An example of application in robotics can be observed in DeepMind project (Gu et al., 2017) where reinforcement learning is used for robot to generate adaptive control system that learns from its past experience and behaviour. Autonomous driving can also be included in this category. Companies such as Tesla and

Waymo are already implementing this technology to their cars with hope to improve road safety.

Some of the most successful results of this particular field include the victories of computer against human in game of chess and Go. In 1997, Deep Blue, an IBM supercomputer, defeated world champion Garry Kasparov in a rematch game after initially losing in 1996. However, a more interesting story happened rather recently in 2016 when Google Deepmind's AlphaGo beat Lee Sedol in Go, an ancient Chinese board game. It is said that this victory is more meaningful to the AI community since Go has a lot more possible moves compared to the number of atoms available in the universe, a number believed to be impossible to compute using classical methods, making it way more difficult for the machine to learn and master the game.

Reinforcement learning is also used to beat video games such as ATARI games, Super Mario and others. Video games bots are commonly used to practice reinforcement learning since it is way cheaper than using machines or robots in real world. The key to success in this field is to have a clear output or end goal. In Mario, the goal for the bot is to reach the end of the game by jumping obstacles and defeating enemies, which is a really clear goal. But in some other games, especially open world games like Pokémon and Legend of Zelda, there are multiple of goals and options to be achieved. This is where bots could not do well yet because as of now, they can only handle one specific task at a time.

3.3 Machine learning algorithms

There are huge number of machine learning algorithms available, ranging from the simplest simple linear regression to the highly complex artificial neural network. Each and every one of the algorithm has its own strengths and weaknesses. There is no one algorithms that will work best for all problems. For instance, linear regression is very easy to interpret on how the decisions are made, but is limited to linear relationship, thus low performance for non-linear data. Artificial neural network is able to achieve state-of-the-art performances on many datasets, both linear and non-linear, but at the same time it is not very easy to interpret. Some even consider it as a black-box where only input and output are obvious, but the processes in the middle are not. For this research, interpretability is more important than performance since the work wants to bring the information from the model forward for OLED device fabrication.

3.3.1 Random forest

Random forest originated from another algorithm called decision tree. Multiple trees are combined together to become a forest (Breiman, 2001). Combinations of few algorithms together are usually called ensemble models, in which they usually have improved generalization ability and robustness compared to any algorithms by its own. To understand random forest, let's look at a simple example of decision tree, used to classify types of Iris flower in Figure 3.5. In this example, petal length and width are used to classify such flowers. In the first level, flowers with petal length less than 2.45 cm are classified as Setosa, and flowers measuring more than 2.45 cm need to go through the second level of the decision tree. Here, the petal width is used to decide whether the flower is Versicolor or Virginica.

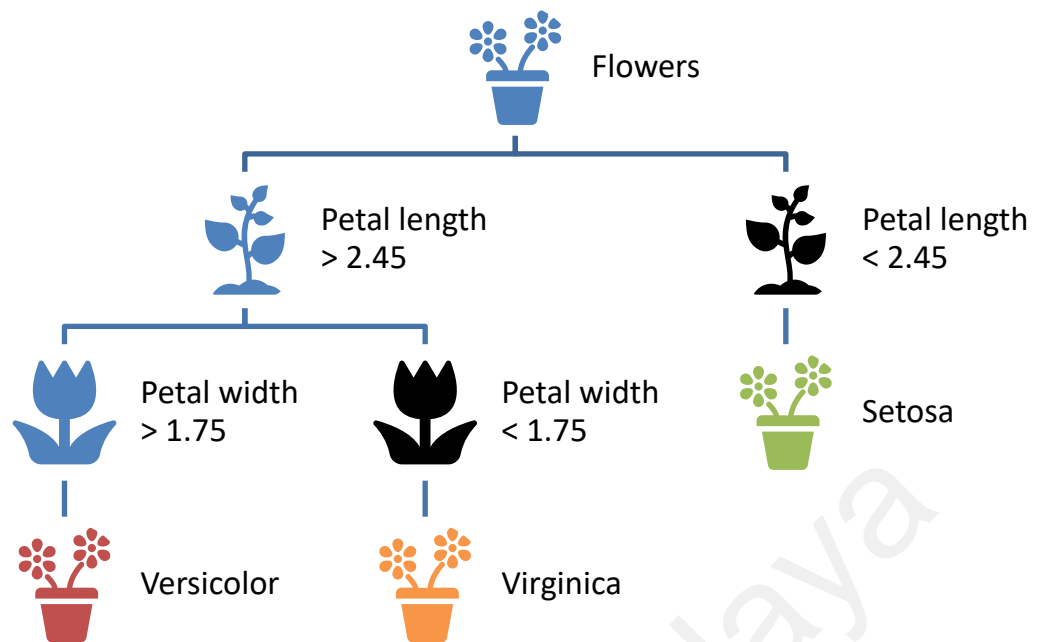


Figure 3.5: Example of decision tree used to classify Iris flowers based on their petal length and width.

Random forest selects random subset of the training data for fitting and several number of selections are made for a dataset. For each of the subset, decision trees are made for the fitting process. On top of that, this algorithm also selects randomly the features that are to be used for each fitting. These random selection processes ensure the algorithm is robust and has a great predictive ability. One major advantage of random forest is it has low variance as the result from averaging results from the random subtrees created. The randomization however increases slightly the bias of the model.

In the paper presenting random forest (Breiman, 2001), it is stated that random forest has some desirable characteristics such as good accuracy, robust to outliers and noise, and faster than bagging and boosting method. These advantages are the result from how random forest works, such that random split selection and random feature selection are done for each tree. Another important thing to mention is that randomness used in this algorithm needs to minimize the correlation without reducing the strength. Random forest is one of the methods proven to be capable of handling large numbers of variables even

with comparatively small dataset (Gromping, 2009). Random forest also allows the user to discover the importance of the variable from its feature importance. This will be discussed further in Chapter 5.4.

For regression problems, random forest works by growing trees but the predictor for each tree now takes numerical values as opposed to the class labels for classification problems. The average value of the tree is calculated to produce this predictor. On top of that, random feature selection is utilized together with bagging technique to complete the regressor.

3.3.2 Extreme gradient boosting (XGB)

Extreme gradient boosting algorithm (XGB) or XGBoost originates from another machine learning algorithm called gradient boosting algorithm. Both algorithms are similar in the sense that they use a technique called tree boosting, which is essentially a boosting technique for decision tree. It is described in its original published paper (Chen & Guestrin, 2016) that there are few differences between the two algorithms and some areas where XGB is focusing on:

- Scalable end-to-end tree boosting system
- Parallel and distributed computing for faster computation
- Sparsity aware algorithm – detect sparse data

XGB is said to be sparsity aware that it can handle sparse data set in a very fast fashion. This is not the case for other algorithms where they mainly focus on dense data. Another advantage of XGB is its ability to be computed parallelly. The reason why this technique is used in XGB is because decision tree needs the data to be sorted. This process consumed lots of time especially for large dataset. These steps are then combined to

produce a robust end-to-end machine learning technique capable of handling wide variety of problems.

XGB is one of the most popular algorithms lately, for machine learning practitioners for all sort of machine learning problems. XGB is also the algorithms that wins lots of competitions in Kaggle (Chen & Guestrin, 2016), an online machine learning competition websites. The reason for its popularity is because XGB brings, essentially, the already powerful gradient boosting algorithm to its limit in terms of computation speed and performance.

3.3.3 Adaptive boosting (AdaBoost)

AdaBoost (Freund & Schapire, 1997) is one of the earliest boosting algorithms and typically has a very good performance for machine learning tasks. In AdaBoost, weak learners, features that perform slightly better than random guessing, are tweaked in favour of instances wrongly predicted by the previous predictors. This is done in adaptive manner, hence the name adaptive boosting.

The weak learners are generally are not robust, but as long as they are better than random guessing, the combinations of these weak learners can converge to be a robust classifier or regressor. Another factor that makes AdaBoost a great algorithm is the weightage given to the training samples. For each iteration, the weightage will increase or decrease depending on whether the training samples correctly or incorrectly predicted by the boosted model. AdaBoost has also been proven to improve regression technique (Drucker, 1997).

One downside of AdaBoost is that it is sensitive to noisy data and outliers. This could be coming from lack of random element in this algorithm when splitting is performed.

One way to deal with this problem is to remove the outliers during the data pre-processing. This way, the outliers will not be used for training.

3.3.4 Gradient boosting

Gradient Tree Boosting or Gradient Boosted Regression Trees (GBRT) (Friedman, 2001, 2002) is a generalization of boosting to arbitrary differentiable loss functions. Similarly, to other boosting methods, gradient boosting emphasizes on the use of weak learners to improve existing learner's performance by reducing the error residuals. Gradient boosting is a generalized version of boosting method such that it can cater to different problems as long as the loss functions are differentiable.

Gradient boosting has some advantages over some other algorithms. First, it is very good in handling data with mixed types. Second, gradient boosting has a powerful predictive power and is relevant for both supervised learning types, namely classification and regression problems. Third, this algorithm is robust to outliers due to its robust loss function incorporated within the algorithm (Pedregosa et al., 2011).

However, gradient boosting is not the all perfect algorithms. For the model to handle humongous amount of data, scalability will be an issue. This problem originates from the nature of the algorithm itself, where it utilizes boosting technique that is hardly parallelizable due to its sequential nature.

3.3.5 K-nearest neighbours (KNN)

Nearest neighbour algorithm is one of the simplest to learn and apply. The basic working principle of this algorithm revolves around the distance metrics. Nearest neighbours are obtained by calculating this distance and the points with the shortest distance are considered neighbours. The number of neighbours is one of parameters used

to tune this algorithm. As for the distance metrics, the most common metrics used are Euclidean, Manhattan and Minkowski distance.

K-nearest neighbours works for both regression and classification problems. In classification, a class is determined based on the majority class of neighbouring data points. This is illustrated in Figure 3.6. This figure shows how decision is made when K is set to three. The class of the unknown data point is determined using the majority class of three nearest data points, which in this example, the star. As for regression task, taking the majority class is not possible since the output is a continuous value. Therefore, the mean value of the nearest neighbours is often used to calculate the output.



Figure 3.6: Nearest neighbours for classification, where $K=3$. The closest three neighbours decide the class of unlabelled instance.

There are some downsides that come with this fairly simple algorithm unfortunately. The features need to be scaled prior to using this algorithm since this algorithm calculated the class or value based on distance. This is not a problem for algorithms based on decision trees. One more thing that needed to be done to increase the performance of this algorithm is dimensionality reduction. This is particularly true for data with more than ten features and is usually done as a precautionary step to avoid the curse of

dimensionality (Domingos, 2012). Moreover, nearest neighbour is also considered as lazy learning algorithm in which the calculation is not done until the classification function is called upon. This could result in delay in making prediction, especially when dealing with large number of features.

University of Malaya

CHAPTER 4: METHODOLOGY

4.1 Data collection (Database preparation)

To build a machine learning model, necessary data are collected, processed and formatted with regards to blue PhOLED devices and their efficiency. This chapter provides detailed description of data collected as well as pre-processing methods used before feeding the data into machine learning algorithms. All processes are conducted using Python, an open source, general purpose programming language (Millman & Aivazis, 2011; Oliphant, 2007). Other packages such as Numpy, Pandas, Jupyter notebook and Scikit-learn are also used to assist the data manipulation and machine learning modelling (Kluyver et al., 2016; McKinney, 2010; Pedregosa et al., 2011; Van Der Walt et al., 2011). Sample code for this experiment can be found in Appendix A.

Data of 304 blue PhOLED devices is collected from literature to be further analysed using statistical methods and then fed into machine learning algorithms. The sample data is included in Appendix B and the full dataset can be found at this work GitHub repository, also linked in Appendix B. The papers of the recorded devices were published from the year 2010 up to 2018. The data collected consists of device structure, layer thickness, triplet energy, frontier molecular orbital energy levels and efficiencies. From the devices data collected, over 400 different materials are recorded with different functionality such as charge transport, charge injection, host material and dopants. While some papers included extra details about the device fabricated, such as charge mobility and surface roughness, most of the paper did not report this information. Therefore, only information widely available to majority of the devices are collected. The linear correlation between the features and the current efficiency are calculated using Pearson correlation, which measures the strength and direction of the relationship. The full list of features collected and their correlation with current efficiency are listed in the Table 4.1.

To put a standard in current efficiency data collected, the efficiency of the blue PhOLED devices is collected at 1000 cdm^{-2} . Ideally, the efficiency data used is the external quantum efficiency (EQE, %), but this data is lacking from a big part of the papers, so current efficiency (cdA^{-1}) is used instead. During data collection, missing data for several devices are found. Devices with missing data are removed and excluded from the modelling process. The detailed data pre-processing method is elaborated in the next subchapter.

Table 4.1: Features along with its meaning used for modelling and the linear correlation with respect to device efficiency.

No.	Features Abbreviation	Feature description	Unit	Linear Correlation with efficiency
1.	homo_ETL1	HOMO level for 1 st electron transport layer from cathode	eV	0.36
2.	total_ETL_thickness	Total thickness of electron transport layer (ETL1 + ETL2 if present)	nm	0.35
3.	thickness_ETL2	Thickness of electron transport layer 2	nm	0.32
4.	homo_ETL2	HOMO level for 2 nd electron transport layer from cathode	eV	0.26
5.	triplet_HTL	Triplet energy of hole transport layer next to EML	eV	0.25
6.	triplet_ETL	Triplet energy of electron transport layer next to EML	eV	0.25
7.	homo_EML	HOMO level for host material in emitting layer	eV	0.23
8.	homo_HTL3	HOMO level for 3 rd hole transport layer from anode	eV	0.23
9.	homo_HTL2	HOMO level for 2 nd hole transport layer from anode	eV	0.23
10.	cathode_workfunction	Cathode work function	eV	0.13
11.	thickness_ETL1	Thickness of 1 st electron transport layer from cathode	nm	0.09
12.	homo_HTL1	HOMO level for 1 st hole transport layer from anode	eV	0.09
13.	lumo_EML	LUMO level for host material	eV	0.08
14.	total_HTL_thickness	Total thickness of all hole transport layer	nm	0.07
15.	thickness_HTL1	Thickness of 1 st hole transport layer from anode	nm	0.07

Table 4.1, continued.

No.	Features Abbreviation	Feature description	Unit	Linear Correlation with efficiency
16.	triplet_HOST	Triplet energy of host material in emitting layer	eV	0.07
17.	thickness_HTL2	Thickness of 2 nd hole transport layer from anode	nm	0.02
18.	lumo_ETL1	LUMO level for 1 st electron transport layer from cathode	eV	0.00
19.	thickness_HTL3	Thickness of 3 rd hole transport layer from anode	nm	-0.01
20.	thickness_HIL	Thickness of hole injection layer	nm	-0.01
21.	homo_HIL	HOMO level for hole injection layer	eV	-0.01
22.	lumo_ETL2	LUMO level for 2 nd electron transport layer from cathode	eV	-0.04
23.	lumo_dopant	LUMO level for emitter	eV	-0.09
24.	thickness_EML	Thickness of emitting layer	nm	-0.12
25.	triplet_dopant	Triplet energy of phosphorescent emitter	eV	-0.16
26.	lumo_HTL3	LUMO level for 3 rd hole transport layer from anode	eV	-0.18
27.	lumo_HTL2	LUMO level for 2 nd hole transport layer from anode	eV	-0.19
28.	dopant_percentage	Phosphorescent emitter percentage in host material	%	-0.20
29.	homo_dopant	HOMO level for emitter	eV	-0.20
30.	lumo_HTL1	LUMO level for 1 st hole transport layer from anode	eV	-0.22
31.	thickness_EIL	Thickness of electron injection layer	nm	-0.27

4.1.1 Descriptive statistics

For every feature collected, the statistics are collected to find insights about the data collected. For instance, triplet energy of dopants collected are quite high with 25% of the data has triplet energy of 2.70 eV or higher. Thickness of cathode_1 in the data on the other hand showed a different property. This layer is also called electron injection layer, and usually consist of very thin layer of the material such as Lithium Fluoride (LiF), Caesium carbonate (Cs₂CO₃) or Calcium (Ca). Based on the data collected, most of the

devices have only few nanometre thick EIL, but some have a thicker layer. This is purely because of the choice of materials used as some materials have insulating property, limiting them to only few nanometre thick (Burin & Ratner, 2000). The distribution for the other features can be found in the Table 4.2.

Table 4.2: Descriptive statistics and distribution of features collected from literature.

No.	Features abbreviation	mean	std	min	25%	50%	75%	max
1.	homo_HIL (eV)	5.92	1.60	4.70	5.20	5.20	5.30	9.70
2.	thickness_HIL (eV)	21.75	20.42	0.00	3.00	10.00	40.00	60.00
3.	lumo_HTL1 (eV)	2.39	0.52	1.75	2.00	2.40	2.50	5.80
4.	homo_HTL1 (eV)	5.39	0.53	1.90	5.20	5.50	5.50	9.70
5.	thickness_HTL1 (nm)	33.70	22.30	0.00	20.00	30.00	50.00	85.00
6.	lumo_HTL2 (eV)	2.43	0.49	1.75	2.00	2.40	2.40	5.80
7.	homo_HTL2 (eV)	5.59	0.45	1.90	5.50	5.70	5.90	6.10
8.	thickness_HTL2 (nm)	4.57	5.74	0.00	0.00	0.00	10.00	30.00
9.	lumo_HTL3 (eV)	2.43	0.49	1.60	2.00	2.40	2.40	5.80
10.	homo_HTL3 (eV)	5.59	0.45	1.90	5.50	5.70	5.90	6.10
11.	thickness_HTL3 (nm)	0.13	0.99	0.00	0.00	0.00	0.00	10.00
12.	total_HTL_thickness (nm)	38.46	23.71	0.00	25.00	40.00	50.00	110.00
13.	triplet_HTL (eV)	2.51	0.99	0.00	2.82	2.87	3.00	3.14
14.	lumo_EML (eV)	2.38	0.34	1.62	2.19	2.40	2.50	5.80
15.	homo_EML (eV)	5.92	0.50	2.20	5.66	5.90	6.10	7.53
16.	triplet_HOST (eV)	2.87	0.16	2.08	2.75	2.89	2.97	3.50
17.	thickness_EML (nm)	26.70	12.05	10.00	20.00	25.00	30.00	70.00
18.	lumo_dopant (eV)	2.95	0.20	2.20	3.00	3.00	3.00	3.16
19.	homo_dopant (eV)	5.69	0.21	4.80	5.70	5.70	5.70	6.27
20.	triplet_dopant (eV)	2.71	0.05	2.54	2.70	2.70	2.70	2.90

Table 4.2, continued.

No.	Features abbreviation	mean	std	min	25%	50%	75%	max
21.	dopant_percentage (%)	9.93	3.97	0.00	8.00	10.00	12.00	30.00
22.	triplet_ETL (eV)	2.83	0.25	2.43	2.70	2.75	2.80	3.40
23.	total_ETL_thickness (nm)	38.19	10.53	5.00	35.00	40.00	45.00	90.00
24.	lumo_ETL1 (eV)	2.72	0.23	2.20	2.52	2.73	2.80	3.50
25.	homo_ETL1 (eV)	6.55	0.32	5.30	6.30	6.68	6.68	7.50
26.	thickness_ETL1 (nm)	1.42	4.20	0.00	0.00	0.00	0.00	30.00
27.	lumo_ETL2 (eV)	2.76	0.23	2.20	2.73	2.73	2.80	3.50
28.	homo_ETL2 (eV)	6.52	0.33	5.30	6.20	6.68	6.68	7.50
29.	thickness_ETL2 (nm)	36.30	10.28	3.00	30.00	35.00	40.00	80.00
30.	cathode_workfunction (eV)	3.37	0.38	2.20	3.50	3.50	3.50	4.30
31.	thickness_cathode1 (nm)	1.72	2.58	0.00	1.00	1.00	1.00	15.00
32.	Current efficiency (cd/A)	25.28	14.14	0.00	13.61	23.72	35.40	64.38

4.1.2 Data exploration

Based on the data collected, this work performed an exploration to better understand the data. Firstly, the distribution of each of the collected data is checked. Most of the data collected have normal distribution, except a few. The ones that did not have a normal distribution could be caused by the small sample size that is available. The target feature for our model, current efficiency at 1000 cd/A, has a normal distribution. Some features like thickness of emitting layer and LUMO HTL 3 are observed to have normal distribution, while some other features such as thickness HIL and LUMO HTL 1 does not seem to be normally distributed.

When there are two major materials used for a certain layer, the data will be concentrated along the two materials, and does not follow normal distribution. This

phenomenon is clear with thickness HTL 2 and cathode work function. For cathode work function, which refers to the work function of the buffer layer (if exist) or the cathode itself, there are two major materials used. The majority is lithium fluoride (LiF) which is concentrated at the 3.5 eV and the others are 8-Hydroxyquinolinolato-lithium (LiQ) and Calcium which has the work function of 2.8 eV.

From the correlation table in Table 4.1 and heatmap in Figure 4.1, it is seen that there is no one feature having a very strong linear relationship with the target variable with respect to the current efficiency. This could mean that the relationship between the feature is non-linear exhibiting of complex relation. The heatmap in Figure 4.1 also shows a strong linear relationship between features from the second- and third-hole transporting layer, and to both electron transport layer. The simple explanation behind this is there is a lot of device without the third HTL and second ETL. So, the value for this layer is filled using the value for the neighbouring ETL or HTL respectively while setting the thickness zero. This method is used to ensure the continuity of the layers in the devices and preventing gap between the layers.

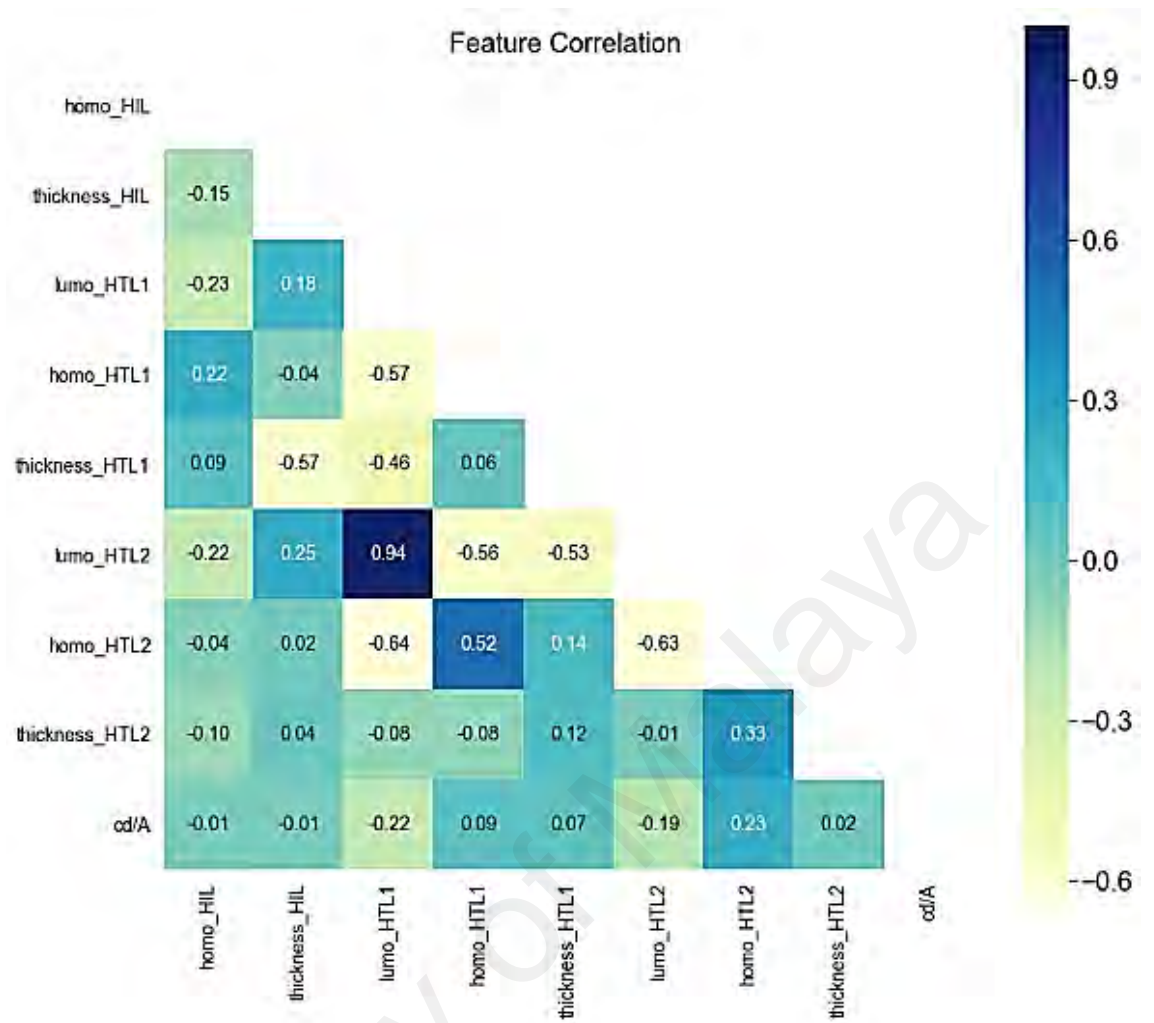


Figure 4.1: Correlation between the features used in the modelling. The heatmap is broken down into four parts for better visualization.

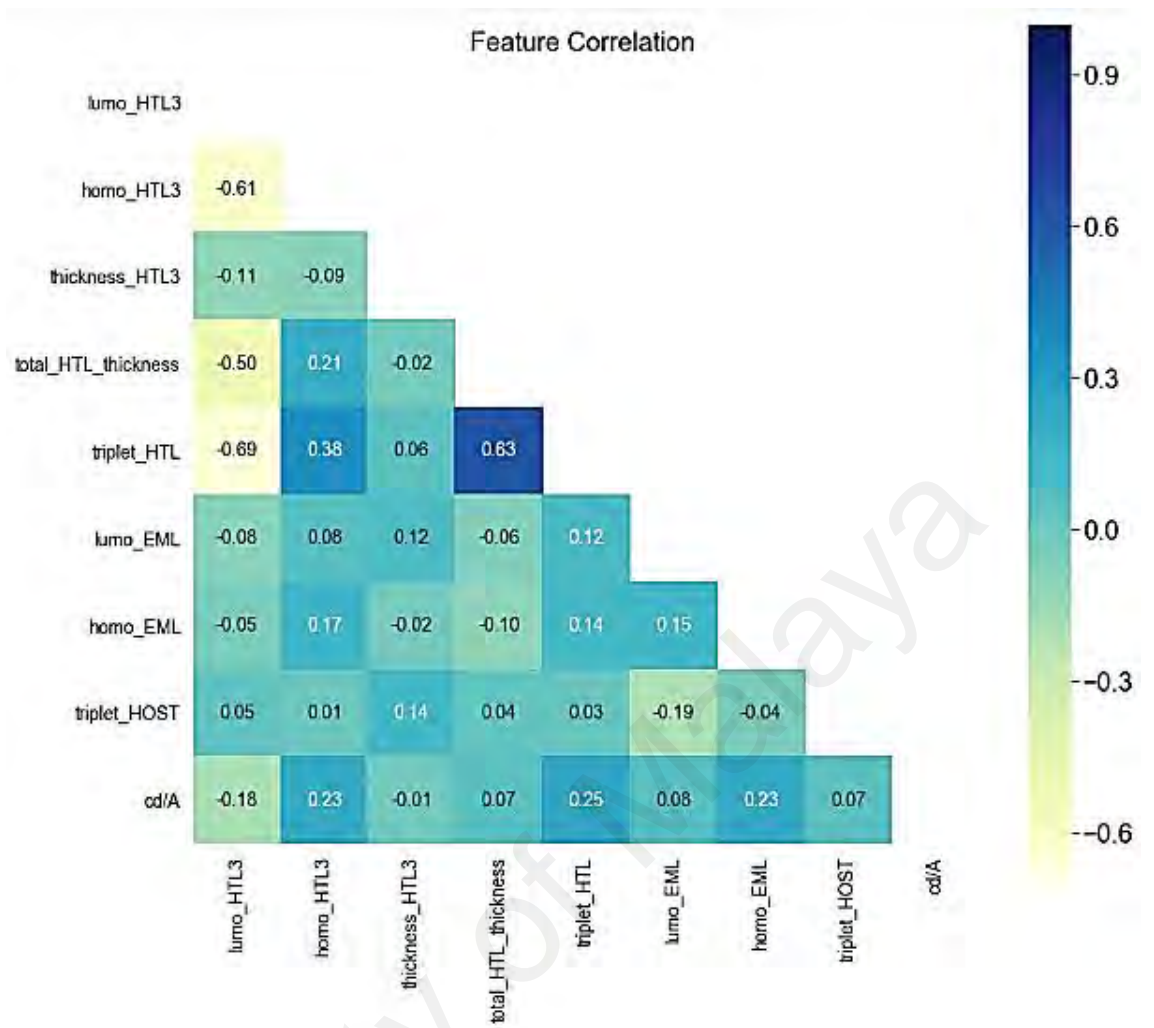


Figure 4.1, continued.

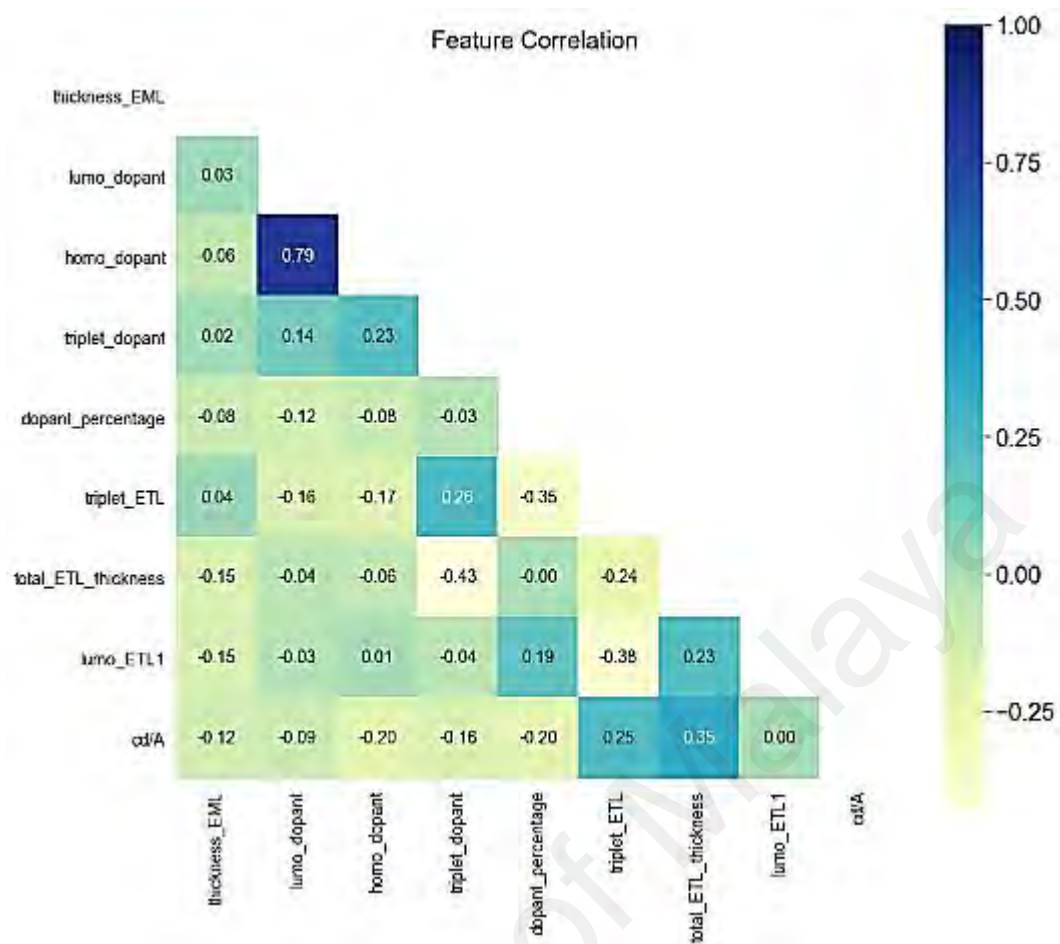


Figure 4.1, continued.

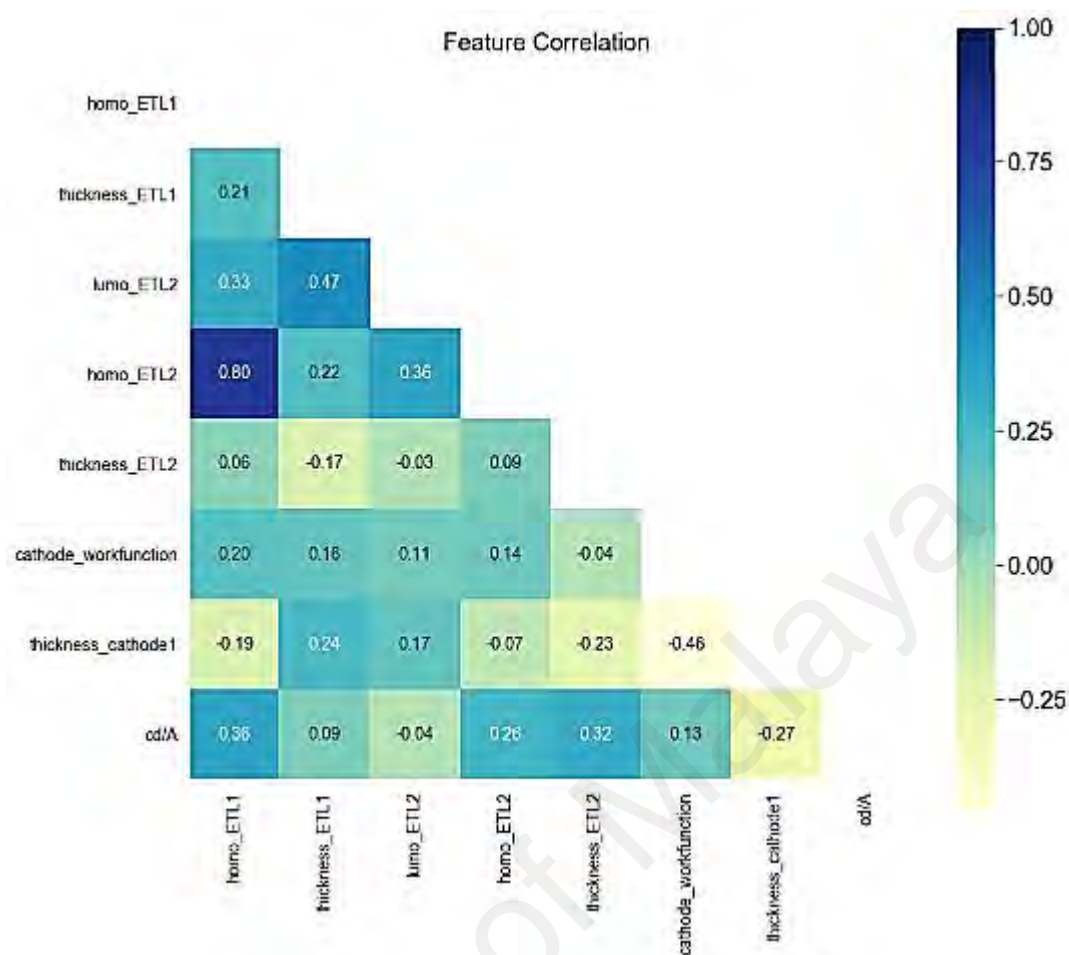


Figure 4.1, continued.

4.2 Data pre-processing

Pre-processing is the heart of any machine learning application. The raw data collected is usually not ready for machine learning. In fact, most of data science works revolve around preparing the data for algorithms, and feature engineering is deemed to be of utmost importance (Domingos, 2012). Firstly, all data need to be converted to numerical value. This means, all information from the layer need to be extracted out in numeric form. One of the main problem is the missing data, since machine cannot be trained on missing values (Kelleher et al., 2015). This can happen because of many reasons. For this case, some papers did not report the certain properties of a particular material such as triplet energy, LUMO or HOMO. If the same materials are reported in other publications,

the value can be used. If it is not found anywhere else, the device is removed from modelling process.

For the same material, it is possible to have several different values due to the different type of measurements done or different instrument used. Therefore, one value is used instead. This is to ensure the correctness of the model built later. Different values could be hard to differentiate between the materials.

Another pre-processing is needed to deal with the difference in the number of layer. The first idea is to fill the missing layer with zeroes. The problem with this approach is that it will introduce layer with zero eV HOMO and LUMO which does not seem to make any sense. So, the layer is replaced with the neighbouring transport layer but the thickness of this layer is set to zero. The accompanying Figure 4.2 shows how the layer replacement is being done. This process mimics the Transfer-Matrix method in optics where the continuity conditions are preserved across layers.

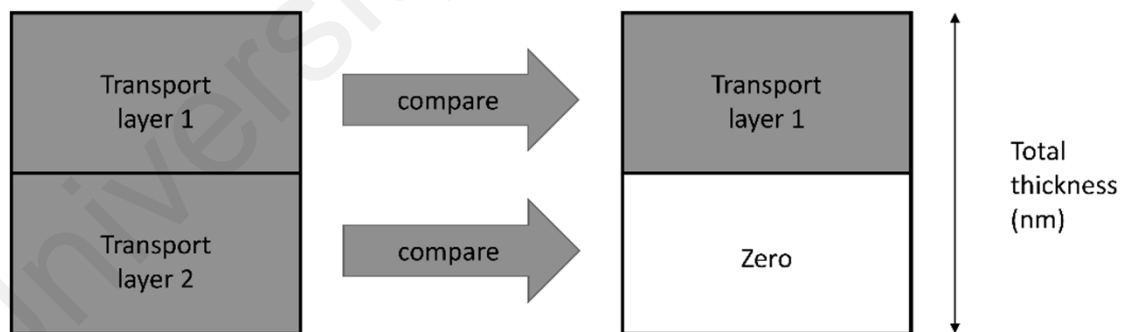


Figure 4.2: Technique used to deal with device with different number of layers.

Some machine learning algorithms require the data to be scaled prior to the fitting process. Scaling is usually done to the continuous features to give same weightage to all the features, and this is particularly important for distance-based algorithms like k-nearest neighbours, linear regression and neural network. As for random forest and other tree-based algorithm, no scaling is needed since the algorithms split the dataset based on a

threshold value of that particular feature. Scaling the data would not really have any significant impact on model performance.

4.3 Features selection

There are a lot of features investigated during device fabrication. But most of the time, only parts of the data reported. This then led to missing data for a particular column, and there might be several missing features for a single device. While it is very enticing to just dismiss the feature with lots of missing value, further understanding of how the mechanism of the device works is very important. For instance, thickness_HTL3 is missing most of the time. However, this layer could be very useful for the device employing this layer. The reason is that, additional transport layer contributes to important functionalities such as lowering energy barrier for charge injection between electrodes and emitting layer. Therefore, it might not be a good idea to drop this feature.

Features based on available data collected, such as triplet HOMO and LUMO. New features are also introduced such as total ETL thickness and HTL thickness, which combine the thickness all of electron transport layers and hole transport layers respectively in a single device. From here, this work can also create another features such as energy difference between each consecutive layers and so on. The only problem here is that the data collected is quite small, limiting the number of features. Increasing the number of features used without increasing the data collected might introduce the curse of dimensionality. Furthermore, when there is a lot of missing value on the new features, this would turn the dataset into a sparse dataset, which could be problematic for some machine learning models relying on statistical inference on the features used. So, for now, this research will stick to the current features only.

CHAPTER 5: RESULTS AND DISCUSSION

5.1 Metrics of performance

For a regression problem, there are a few metrics that are commonly used such as mean absolute error (MAE) and mean squared error (MSE). As for our case, two metrics are used to measure the performance of each algorithms of this data. Root mean squared error (RMSE) and coefficient of determination, R^2 . RMSE measures the mean margin of error between the predicted efficiency and real efficiency reported. The formula for both metrics is listed.

$$RMSE = \sqrt{\frac{\sum_{i=1}^n (y'_i - y_i)^2}{n}} \quad (5.1)$$

$$R^2 = \frac{[\sum_{i=1}^n (y - \bar{y})(\hat{y} - \bar{y})]^2}{\sum_{i=1}^n (y_i - \bar{y})^2 \cdot \sum_{i=1}^n (y'_i - \bar{y}')^2} \quad (5.2)$$

where y_i and y'_i represent the measured and predicted values respectively. \bar{y} and \bar{y}' represent the mean value for the measured and predicted value respectively. n is the total number of data.

The metrics are used to evaluate the algorithms based on two sets of data, the test set and the validation set. Before any fitting is done, the data is divided into two mutually exclusive subsets, the training and testing set (also called holdout set). The split is done randomly but a seed is given to the randomization process for reproducibility. Common practice is to divide the data in 3:1 or 2:1 ratio with the bigger portion used for training. The test data is then used to measure the fitting produced by the training set using the metrics mentioned above. As for the validation set, part of the training data (after train-test split) are used for a process known as cross validation. This process will be explained in depth in the next section.

5.2 Cross-validation

Overfitting is one of the main culprits in machine learning. Overfitting occurs during training step, where the algorithm tries to fit to every single data point in the training set. It gives great result when tested on training set, but when tested on new, unseen dataset, the model fails to produce sufficient generalization and hence lead to bad performance. This problem can also happen when the model tried to get the best result on validation set or test set, it could also overfit to that particular dataset. Underfitting on the other hand, generally means that the model did not learn enough in a sense that it could not find the right generalization for the function. Underfitting can be eliminated by few means, for instance, hyperparameter tuning and feature scaling. Overfitting and underfitting can be better understood by looking at Figure 5.1.

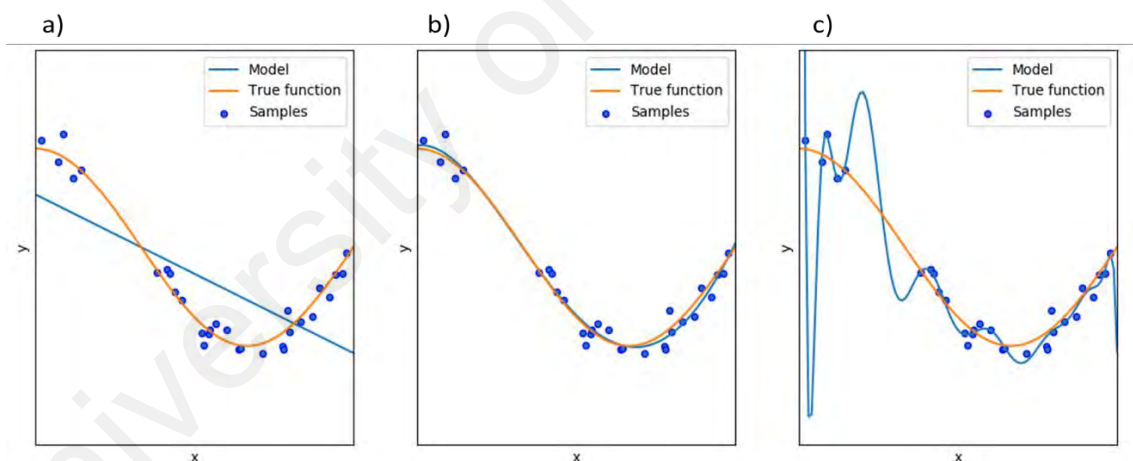


Figure 5.1: Examples of a) underfitting, b) nice fitting and c) overfitting.

Cross validation is a technique used to test the fit produced by each model. The concept is similar to holdout test set, but it is more robust. First, the whole training set is divided into k-fold, where k is an integer, usually 3, 5 or 10 depending on size of data. One part of the fold is then excluded from training and is used for testing. Then, the same procedure is repeated using the other parts of the fold. The error is calculated for each testing and the average performance is calculated. This is why it is more robust than the normal hold

out test set. This method is also proven to be very efficient to avoid overfitting to either training set or testing set. Figure 5.2 provides an illustration to help understanding this process.

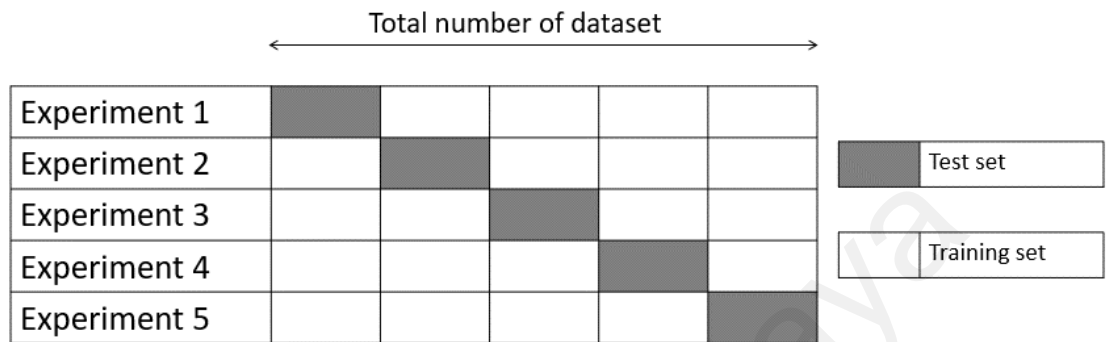


Figure 5.2: Cross validation example using k-fold, where $k = 5$. The testing and training data are changed for every experiment.

This example shows a five-fold experiment, in which the data is divided into five equal parts. The white parts are used for training and the grey is used for testing. In each iteration, the training and testing set is changed to make sure the model does not overfit to any single training or testing set.

5.3 Performance of models

Multivariate regression models were developed based on 31 features and 304 devices data. The predictive power of the model was tested using two validation techniques, hold-out validation and k-fold cross validation. The performances of the models are recorded both on the holdout test set and also on the mean of the cross validations on both of the metrics mentioned earlier, RMSE and R^2 . The result for five different machine learning models is shown in Table 5.1.

Table 5.1: Performance of different machine learning models on cross validated training data and test set. Bold shows the best result.

Models	Cross validated R ² mean	Cross validated RMSE mean (cd/A)	R ² on test set	RMSE on test set (cd/A)
Random forest	0.67	7.502	0.73	7.819
XGBoost	0.63	8.314	0.67	8.668
AdaBoost	0.46	10.041	0.60	9.500
Gradient Boosting	0.65	8.167	0.68	8.464
K-Neighbors	0.37	10.530	0.38	11.826

The results showed that random forest has superior performance compared to the other algorithms in all of the metrics used, with R² (Equation 5.1) of 0.67 on the cross validation mean score, and 0.73 on the test set. Its RMSE score (Equation 5.2) is also the lowest with 7.502 and 7.819 cd/A on the cross-validated score and test score respectively. This score is followed by algorithms using boosting techniques, gradient boosting and XGBoost. K-nearest neighbours performed worst among the chosen algorithms, barely achieving 0.4 on the R² scores for both mean cross validation and on test set and also had over 10.0 cd/A RMSE on both sets.

To visualize the result of the random forest fitting, a graph of predicted current efficiency versus true current efficiency is plotted in Figure 5.3. The figure shows that the predicted efficiency agrees with the true efficiency for most of the devices, in both training and testing datasets, but few outliers are still observed in the test set predictions. Insufficient generalization of random forest algorithm can result in these outliers and affect the R² score.

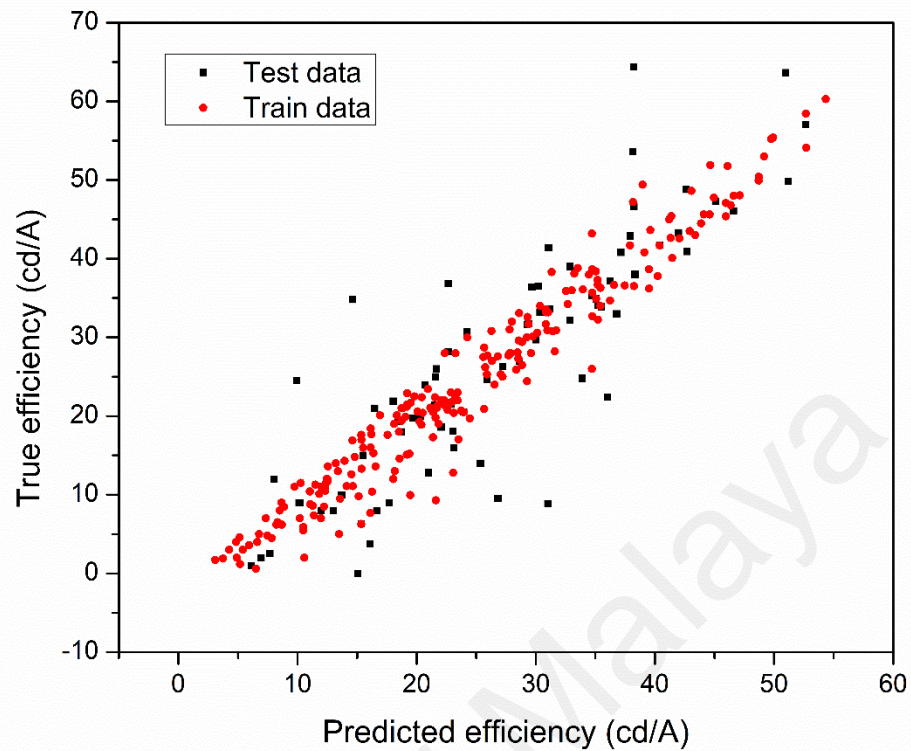


Figure 5.3: Plot of predicted device efficiency versus true experimental efficiency using random forest regression algorithm. The true efficiency is the current efficiency of devices measured at 1000 cdm^{-2} . X-axis is the predicted efficiency and y-axis is the true experimental value.

Dataset size used could be one of the reasons why random forest scored the highest as mentioned in Chapter 3.3.1 earlier. Every other algorithm has its own advantages and disadvantages, in fact there is a theorem called ‘no free lunch’ theorem. To be used in machine learning context, it translates to, no one algorithms is the best for all ML problems, and each problem requires specific tunings of hyperparameter to get the best result. While some of the algorithms performed poorly in this dataset, it does not mean that the algorithm is bad, it just meant that random forest fits the dataset better, given the features and the size of the data.

This result obtained is very impressive considering the low amount of data collected and the high features in the dataset. Since different sizes of training and testing sets can affect the overall performance, this study performed another experiment with different

combinations of the training and testing sets to study the effect. It shows that the more data are employed during the training stage, the better is the model performance. This result is shown in Table 5.2.

Table 5.2: Performance of different machine learning models on different training sizes.

Algorithms	Train : Test ratio	R ²	RMSE (cd/A)
Random Forest	0.75:0.25	0.73	7.819
	0.50:0.50	0.63	8.834
	0.25:0.75	0.33	11.752
XGB	0.75:0.25	0.67	8.668
	0.50:0.50	0.57	9.618
	0.25:0.75	0.20	12.803
AdaBoost	0.75:0.25	0.60	9.500
	0.50:0.50	0.51	10.197
	0.25:0.75	0.23	12.520
Gradient Boosting	0.75:0.25	0.68	8.464
	0.50:0.50	0.59	9.334
	0.25:0.75	0.30	12.003
K-nearest	0.75:0.25	0.38	11.826
Neighbours	0.50:0.50	0.25	12.736
	0.25:0.75	-0.04	14.594

Since random forest achieved the highest R² and the lowest cross validated RMSE mean score, it is selected for further analysis. This algorithm which makes use of weak learners to make a better prediction seems to fit our features and size of the dataset (Géron,

2017). Random forest is also known to handle data with large dimensions/variables even with comparatively small dataset. This could be the reason why it outperformed other algorithms. Since random forest is based on decision trees, the model's path to predicting the efficiency of a device can be traced back using random forest's feature importance. This feature importance is a big help in real world situation and represent a major advantage of tree-based algorithms over neural network. Next sub chapter will discuss more on this matter.

5.4 Feature importance analysis

From our best fitting model, the random forest, a more detailed analysis was made to investigate how the algorithm made each prediction. In Python's Scikit-learn implementation of random forest, an optimized version of classification and regression tree (CART) algorithm is used (Pedregosa et al., 2011). CART works by creating a binary tree in which each node produces two more edges. Afterwards, it will try to discover the best split for the features based on a criterion. The criterion used for node impurity in regression is variance reduction, while for classification, it can be either Gini impurity or twoing criterion (Singh & Gupta, 2014).

In tree-based algorithms, random forest for instance, the decrease in node impurity is calculated as feature importance. The probability of reaching that node is added as weightage to the calculation. Then, to get the node probability, the number of samples that reach that node is divided by total number of samples. Important features are represented by feature with the highest of this value.

The value obtained above is the feature importance for a single decision tree. Then, to calculate the final feature importance for random forest, the average of all trees is calculated that is, importance of each trees is summed up and divided by the total tree

number. The feature importance of our random forest algorithm on the PhOLED data set is shown in Figure 5.4, ranked based on which features is more informative for the algorithm to make decisions.

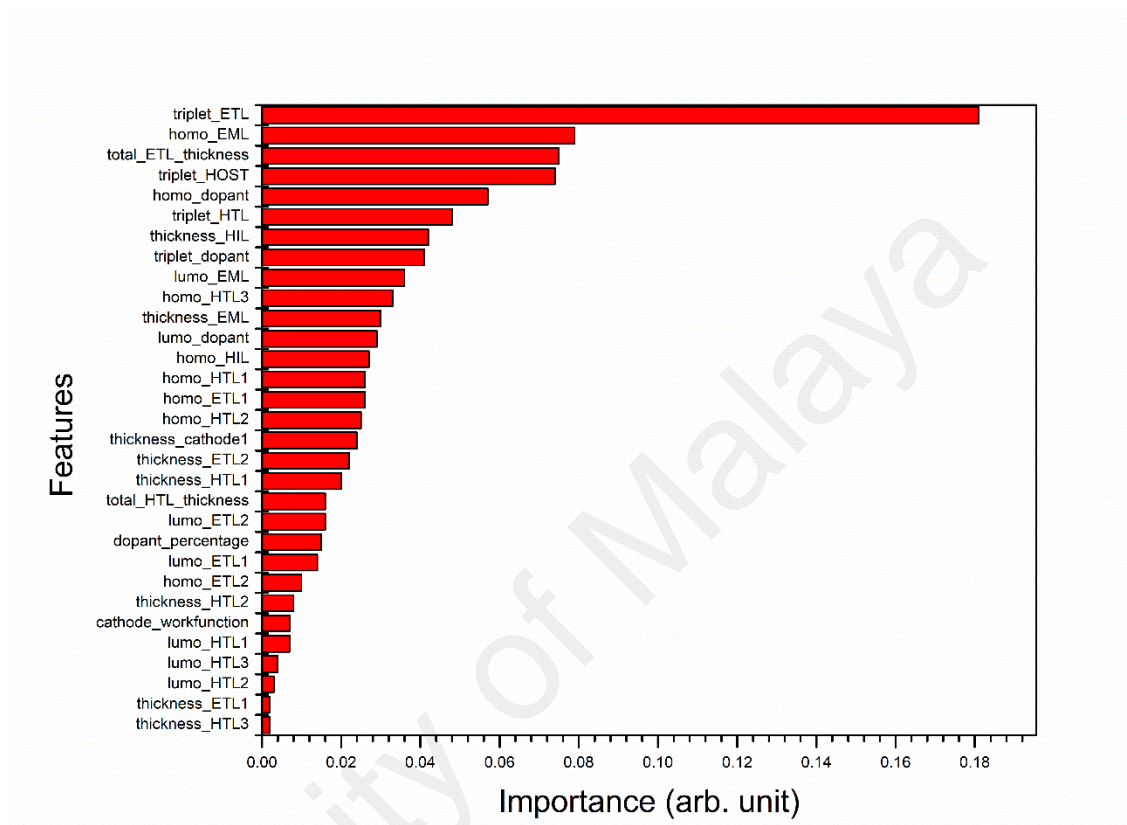


Figure 5.4: Feature importance based on the random forest algorithm.

Triplet energy for ETL is the main factor affecting efficiency of the devices, based on our random forest model. This figure shows that triplet energy of ETL is way more important than the other features, followed by HOMO of EML, total thickness of ETL layer and triplet energy of host, coming at second, third and fourth respectively.

One of the most noticeable features about Figure 5.4 is the position of triplet energy of host material (triplet_HOST). It is widely discussed in publications that triplet energy of host material for blue PhOLED must be high or at least higher than triplet energy of the phosphorescent emitter (Park et al., 2017). This is mainly to prevent the energy to

back transfer from the guest emitter to the host, lowering device efficiency (Woon et al., 2015). Hence, the work takes a look back at the data collected to investigate this matter.

It turned out, in the data itself, most of the devices already had host material with higher triplet energy than the triplet energy of its phosphorescent emitter (triplet_dopant) (Gudeika et al., 2017; Park et al., 2017). The distribution of the two features is plotted in Figure 5.5. The relationship between the two distributions introduced bias in the dataset, which then transferred to the model, causing the triplet energy of host material (triplet_HOST) to be less important to the algorithm. This bias could originate from the source of the data used, in which most of the devices are from publications from the last 5 years.

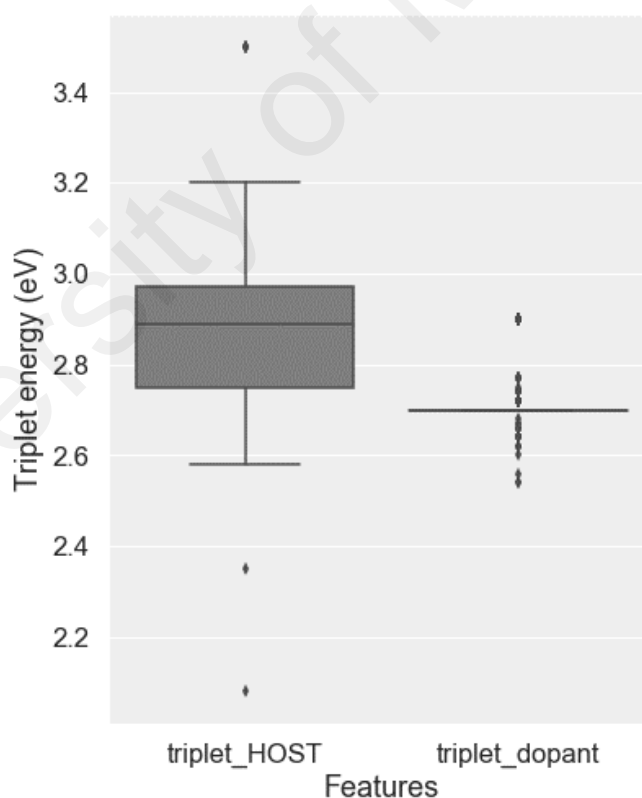


Figure 5.5: Boxplot comparison of data distribution between triplet energy of host material and dopant.

This suggested that most researchers are aware of this important relationship, and deployed materials with higher triplet energy for host material in devices fabricated. In

spite of that, this feature still ranked fourth according to our random forest model, which is still relatively high. It is believed that this feature is still useful in differentiating device efficiency, especially devices that use low triplet host materials.

The requirement of high triplet energy for host material also indicates that electron trapped-limited transport of organic materials does influence the order of importance of device efficiency. Figure 5.6 shows that the current efficiency is almost proportional to the host triplet energy and seems to be saturated at 2.8 eV as extracted from the machine learning model. This figure also suggests that the ideal triplet energy of host materials for triplet excitons confinement for FIrpic needs to be 0.1 eV larger than the guest triplet energy. Host with high triplet energy is needed to prevent backward energy transfer from phosphorescent emitter to host (Hladka et al., 2018; Woon et al., 2015).

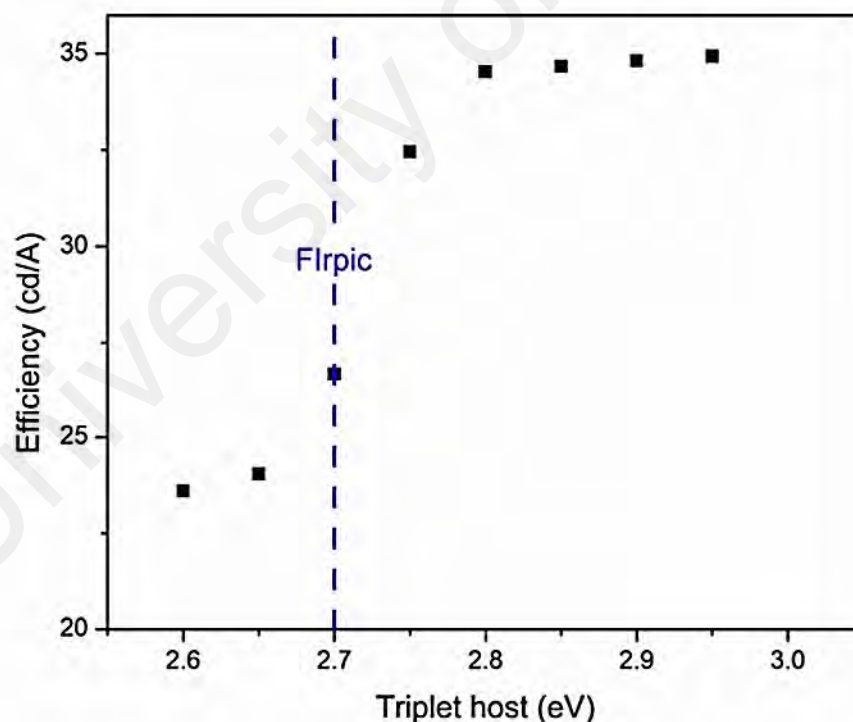


Figure 5.6: Current efficiency of generated blue PhOLED devices with various host triplet energy. Blue line shows the triplet energy for FIrpic.

To further understand the effect of other important features in the rank, this work generated random devices with different values of the selected features for simulation. The features of interest such as triplet energy of EML, ETL and HTL were varied in the simulation, while maintaining other features constant. In the first experiment, EML triplet was fixed at 2.6 eV, 2.8 eV and 3.0 eV, while ETL and HTL triplet is varied between 2.5 eV- 3.0 eV. These features were then used to predict the current efficiency of devices using Random forest algorithm trained in previous section. The result is presented in the contour plot in Figure 5.7 a) - c), where the colour represents device efficiency, ranging from blue to red.

In the second experiment, HOMO level of EML was fixed at 5.6 eV, 5.8 eV and 6.0 eV, while HOMO level of HTL and ETL were varied between 5.2 eV – 6.0 eV and 6.0 eV to 7.3 eV respectively. Then again, the same random forest model is used to predict the devices' current efficiency. The result is presented in the contour plot in Figure 5.7 d) - f), where the colour represents device efficiency, ranging from blue to red. Since the contour plots are generated from the available materials within our collected data, the white regions in the contour plots indicate the lack of materials having such parameters. We do not extrapolate such regions as the model is trained based on available material parameters as accurate extrapolation using machine learning is still in infancy.

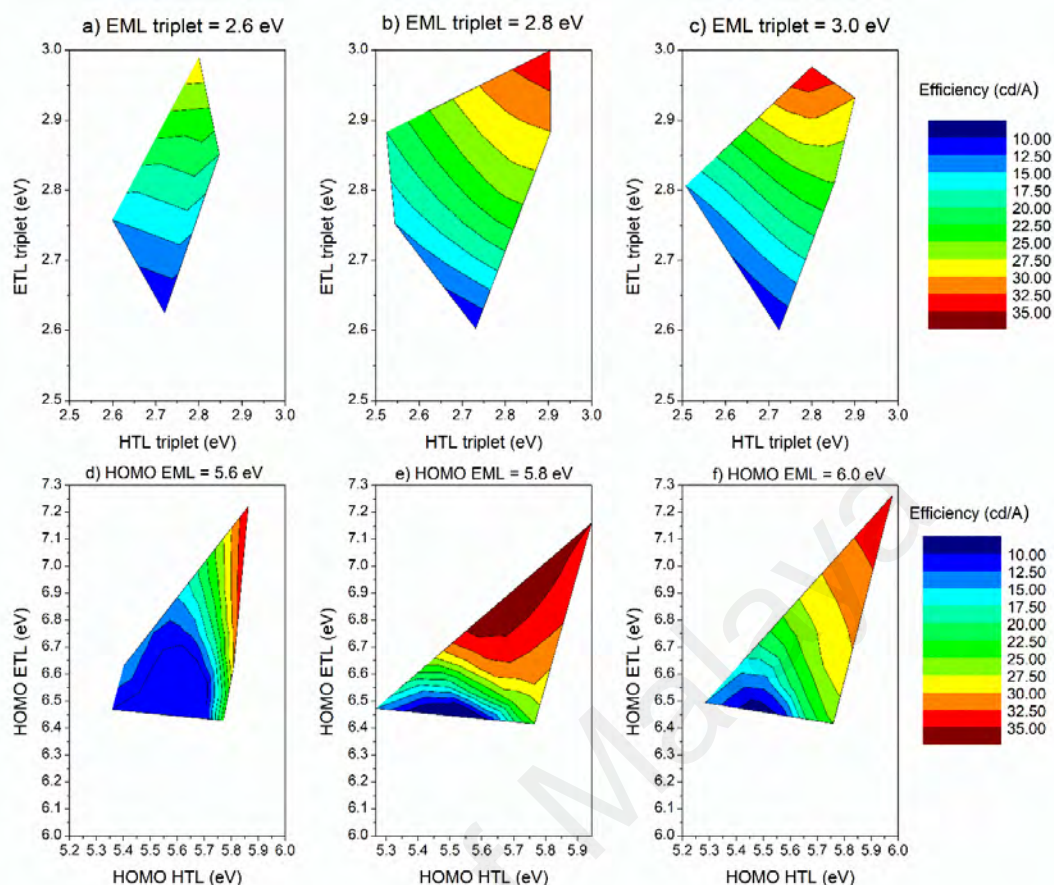


Figure 5.7: Contour plot a) – c) shows the relation between triplet energy of HTL and ETL with device efficiency. EML triplet energy is fixed at 2.60, 2.80, 3.00 eV respectively. Contour plot d) –f) shows relation between HOMO level of HTL and ETL with device efficiency. HOMO level for the host material is fixed at 5.60, 5.80 and 6.0 eV respectively.

The result in Figure 5.7 a) - c) is important for several reasons. One is that now it can be seen that current efficiency increases with triplet energy but not so much with the triplet energy of HTL. Generally, triplet energy of transport layers next to the emitting layer needed to be high to prevent the excitons diffusing into the transport layer and produce nonradiative combination. From the result, only triplet energy from ETL is deemed to be important. This phenomena suggest that the hole has greater mobility than electron in the device which could be coming from electron traps usually found in small molecule and polymer based devices (Nicolai et al., 2012). Since hole current drifts faster, the carrier recombination zone is shifted closer to the electron transport – emitting layer interface (Kuik et al., 2011; Nicolai et al., 2012). If charge recombination occurs at high

density near the ETL, in order to prevent the loss from triplet excitons via Dexter energy transfer to the next layer, high triplet energy is required for the ETL.

Since HOMO EML comes second in Figure 5.4, the result from the second device variation in contour plots d)-f) in Figure 5.7 tell us how this feature affected device efficiency with a fixed emitter (FIRpic). Varying both HOMO level of ETL and HTL seem to have observable changes in current efficiency of the device. Appropriate host HOMO levels are needed to facilitate the charge injection and transport from adjacent layers by reducing the energy barrier needed to be overcome by the charges (Bian et al., 2018). Figure 5.7 d) – f) show the vast region of high efficiency can be found when the triplet energy of EML is 5.8 eV as shown in Figure 5.4 e). It is clear from Figure 5.7 d) and Figure 5.7 f) that having shallower hosts and having FIRpic molecules acting as the charge transporting traps are detrimental to the device efficiency. Energy levels of HTL that match or close to the HOMO level of FIRpic at 5.7-5.8 eV (Chiu et al., 2017; Dong et al., 2017) lower the carrier injection barrier removing carriers accumulation at transport layer-emissive layer interface (Jou et al., 2015). This indicates that the stepwise or graded HTL layers might be beneficial in increasing the device efficiency. Figure 5.7 d) – f) seem to suggest that HOMO levels of ETL must be at least 1 eV deeper than the EML in order to be an effective hole blocker

The next feature in the importance rank is total ETL thickness. To investigate this feature, this work generated device with the same materials, but with different thickness for each layer ranging from 5 nm to 65 nm. The total thickness for the three layers is kept constant at 80 nm. The result is presented in Figure 5.8. From the result presented, it is observed that ETL thickness of at least 30 nm is needed to achieved at least 30 cd/A efficiency. Also, from the figure above, it seems like there is only little effect of changing HTL thickness based on the Random forest interpretation.

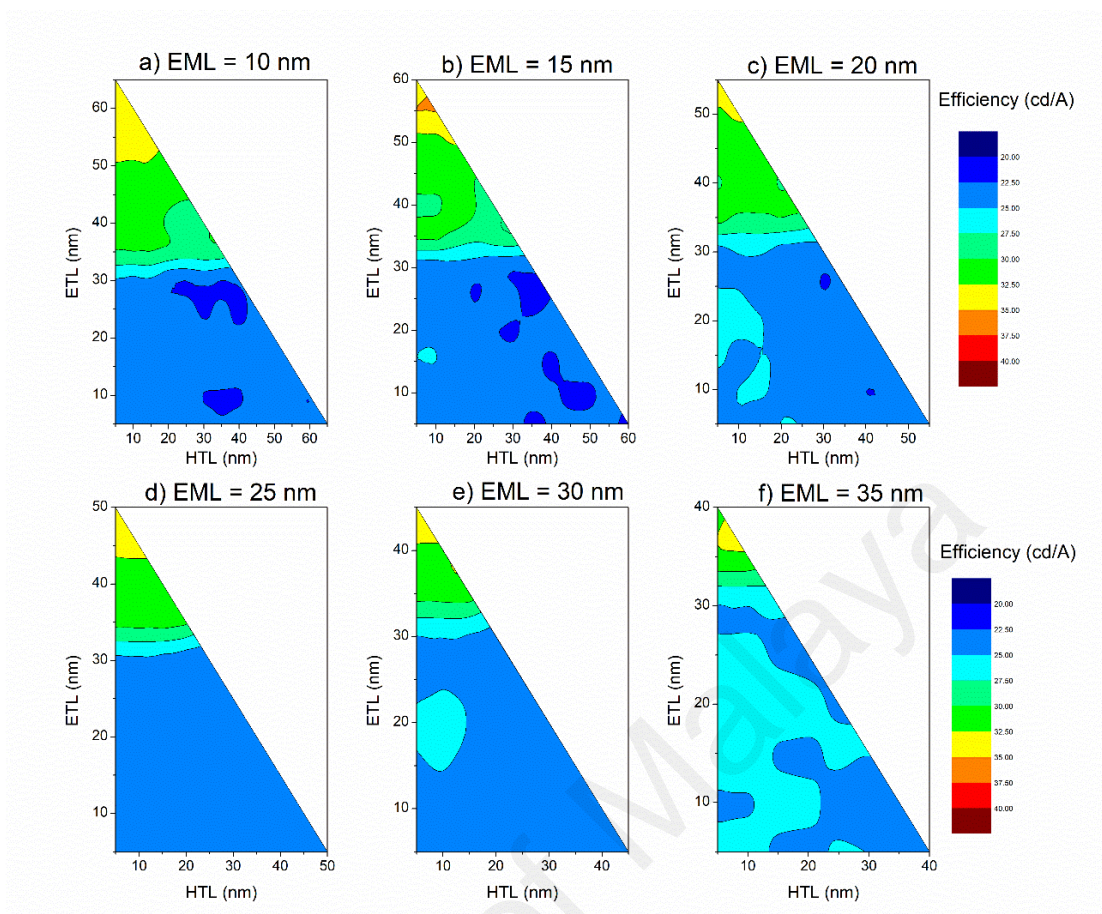


Figure 5.8: Relation between thicknesses of ETL, HTL with the device efficiency. EML thickness increases by 5 nm from a) 10 nm to f) 35 nm.

While the feature importance is based on statistical inference and calculation, it is very useful to show us the way to select materials with certain parameters. To fabricate a blue PhOLED device with at least 35 cd/A current efficiency, the triplet energies of the ETL, host and HTL must be at least 2.95 eV, 2.8 eV and 2.8 eV respectively and the HOMO levels for the HTL, EML and ETL should be at least 5.8 eV, 6.0 eV and 6.7 eV deeper respectively using FIrpic as the emitter. For the LUMO levels the ETL and EML should be in the range of 2.6–2.7 eV and 2.4–2.5 eV respectively. The thickness of each layer is also critical with ETL thickness must be at least 30 nm in order to obtain reasonable efficient blue PhOLEDs. These parameters extracted from machine learning should enable synthetic chemists along with quantum molecular modelling to target materials with appropriate parameters, as well as the device scientists to engineer extremely efficient blue PhOLED devices.

CHAPTER 6: CONCLUSION

This chapter provides the summary of the research work done on the feasibility of using machine learning algorithm to predict the efficiency of PhOLED. This chapter briefly discusses the techniques used in this project. Recommendations and ideas for future works are also included in this chapter.

6.1 Summary

The goal of this research is to increase the efficiency of blue PhOLED devices. Instead of taking the usual route of experimentation, which includes material synthesis, design of device architecture, and some few other methods, this work utilized statistical analysis approach which involves machine learning algorithms and techniques. In order to achieve the goal stated, this proposed work determined the features that affect device efficiency the most, and observe how these features impact device efficiency.

Firstly, this work described the mechanism of PhOLED and how each layer in a device functions for a device to emit light. The working principle and details of each and every layer is also included to understand the process. Then, the problems faced by blue PhOLED specifically are discussed and how researchers are tackling this problem.

Secondly, the work dived into machine learning. History of machine learning was described briefly in Chapter 3 as well as the different types of machine learning and their use case in today's world. Then, this work discussed about the machine learning algorithms that were being used for this research. The process behind each algorithm was included, along with their advantages and disadvantages for comparison.

Next, data collection method is discussed along with the pre-processing method before the data is fed into machine learning algorithms. Here, the source of the data and the

features are discussed as well as the rationale of why specific techniques are used when pre-processing the data.

Lastly, the experimental results in Chapter 5 are compiled to compare the performance of different algorithms. From the results obtained, it is concluded that random forest performed the best and further studies are done to see how decisions are made in determining device efficiency. This work learnt that high triplet energy of ETL is among the important features determining the current efficiency of blue PhOLED devices, implying the prevalence of deep electron traps within the current materials.

The results from the random forest model and simulations narrow down quantitatively the material and device parameters that are required to obtain blue PhOLEDs with efficiency > 35 cd/A. We expect that these parameters would be useful in guiding organic chemists and device engineers in making high performance devices. The result also shows that we managed to achieve our objectives to predict device efficiency and to predict crucial factors impacting current efficiency of a blue PhOLED device.

6.2 Future work and recommendation

In this section, recommendations to improve the blue PhOLED device using machine learning techniques for future works are provided. Firstly, in order to continue working on machine learning, more data should be collected. This is because more data points often beat more complex algorithms in machine learning areas. Once more data is obtained, it is possible to play around with feature selection, adding some more features that are believed to play important roles in determining device efficiency. Clever feature selection has been proven to be a huge factor in boosting model performance, which does not necessarily rely on one's background knowledge on that particular field.

Moreover, when the dataset collected is big enough, experimentation with complex algorithm such as artificial neural network can be done. This algorithm has been used widely in real life application following its high performance in vast areas, including image recognition and natural language processing. Another way to build high performance model is by combining multiple algorithms and use them together. This can be done through multiple ways such as stacking, voting and bagging techniques.

Another important thing to add is that this model assumed the alignment of vacuum level across an interface while in the real devices, this is not often the case. Vacuum level shift often occurs at organic/metal or organic/organic as the result from interfacial dipole formation. In fact, this shift can occur up to few eV such as often found in transition metal oxides/organic interfaces, providing a major challenge to the model . Therefore, in future, reporting the vacuum level shift across various interfaces in the literature for a given device should help in building a machine learning model with a higher predictive accuracy, so that superior device can be developed.

Lastly, to extend this idea of improving OLED device by using machine learning, it is possible to change the target variable to something else, such as quantum efficiency and even the CIE coordinates or the spectrum width. This work also recommends applying this technique to other OLED technologies as well such as TADF and fluorescent OLED to get the best result.

REFERENCE

- Baldo, M. A., O'Brien, D. F., You, Y., Shoustikov, A., Sibley, S., Thompson, M. E., & Forrest, S. R. (1998). Highly efficient phosphorescent emission from organic electroluminescent devices. *Nature*, *395*(6698), 151-154.
- Bernanose, A. (1955). Electroluminescence of organic compounds. *British Journal of Applied Physics*, *6*(S4), S54.
- Bian, C. L., Wang, Q., Ran, Q., Liu, X. Y., Fan, J., & Liao, L. S. (2018). New carbazole-based bipolar hosts for efficient blue phosphorescent organic light-emitting diodes. *Organic Electronics*, *52*, 138-145.
- Breiman, L. (2001). Random forests. *Machine Learning*, *45*(1), 5-32.
- Burin, A. L., & Ratner, M. A. (2000). Exciton migration and cathode quenching in organic light emitting diodes. *Journal of Physical Chemistry A*, *104*(20), 4704-4710.
- Chen, T., & Guestrin, C. (2016). Xgboost: A scalable tree boosting system. In *Proceedings of the 22nd ACM SIGKDD International Conference on Knowledge Discovery and Data Mining* (pp. 785-794). San Francisco, CA. ACM.
- Chiu, T. L., Chen, H. J., Lin, T. C., Gau, H. J., Hsieh, Y. H., Huang, J. J., ... Leung, M. K. (2017). Colour stability of Blue-Green and white phosphorescent organic light-emitting diode employing a 9-(2-(4,5-diphenyl-4H-1,2,4-triazol-3-yl)phenyl)-9H-carbazole host. *Dyes and Pigments*, *141*, 463-469.
- Choulis, S. A., Mathai, M. K., & Choong, V.-E. (2006). Influence of metallic nanoparticles on the performance of organic electrophosphorescence devices. *Applied Physics Letters*, *88*(21), Article#213503.
- Djurovich, P. I., & Thompson, M. E. (2007). Cyclometallated organoiridium complexes as emitters in electrophosphorescent devices. In *Highly Efficient OLEDs with Phosphorescent Materials* (pp. 131-161). Weinheim. Wiley-VCH.
- Domingos, P. (2012). A few useful things to know about machine learning. *Communications of the ACM*, *55*(10), 78-87.
- Dong, Q. C., Tai, F. F., Lian, H., Chen, Z., Hu, M. M., Huang, J. H., & Wong, W. Y. (2017). Thermally stable bipolar host materials for high efficiency phosphorescent green and blue organic light-emitting diodes. *Dyes and Pigments*, *143*, 470-478.
- Drucker, H. (1997). Improving regressors using boosting techniques. In *International Conference on Machine Learning* (pp. 107-115). London, UK. Springer-Verlag.
- Forrest, S. R., Bradley, D. D., & Thompson, M. E. (2003). Measuring the efficiency of organic light-emitting devices. *Advanced Materials*, *15*(13), 1043-1048.

- Freund, Y., & Schapire, R. E. (1997). A decision-theoretic generalization of on-line learning and an application to boosting. *Journal of Computer and System Sciences*, 55(1), 119-139.
- Friedman, J. H. (2001). Greedy function approximation: A gradient boosting machine. *Annals of Statistics*, 1189-1232.
- Friedman, J. H. (2002). Stochastic gradient boosting. *Computational Statistics & Data Analysis*, 38(4), 367-378.
- Géron, A. (2017). Hands-on machine learning with Scikit-Learn and TensorFlow: Concepts, tools, and techniques to build intelligent systems. O'Reilly Media.
- Granström, M., & Inganäs, O. (1996). White light emission from a polymer blend light emitting diode. *Applied Physics Letters*, 68(2), 147-149.
- Gromping, U. (2009). Variable importance assessment in regression: Linear regression versus random forest. *American Statistician*, 63(4), 308-319.
- Gu, S., Holly, E., Lillicrap, T., & Levine, S. (2017). Deep reinforcement learning for robotic manipulation with asynchronous off-policy updates. In *The 2017 IEEE International Conference on Robotics and Automation (ICRA)* (pp. 3389-3396). IEEE.
- Gudeika, D., Norvaisa, K., Stanislovaityte, E., Bezikonny, O., Volyniuk, D., Turyk, P., ... Grazulevicius, J. V. (2017). High-triplet-energy derivatives of indole and carbazole as hosts for blue phosphorescent organic light-emitting diodes. *Dyes and Pigments*, 139, 487-497.
- Helfrich, W., & Schneider, W. (1965). Recombination radiation in anthracene crystals. *Physical Review Letters*, 14(7), 229-231.
- Hladka, I., Lytvyn, R., Volyniuk, D., Gudeika, D., & Grazulevicius, J. V. (2018). W-shaped bipolar derivatives of carbazole and oxadiazole with high triplet energies for electroluminescent devices. *Dyes and Pigments*, 149, 812-821.
- Im, Y., Byun, S. Y., Kim, J. H., Lee, D. R., Oh, C. S., Yook, K. S., & Lee, J. Y. (2017). Recent progress in high-efficiency blue-light-emitting materials for organic light-emitting diodes. *Advanced Functional Materials*, 27(13), Article#1603007.
- Jabbour, G., Kawabe, Y., Shaheen, S., Wang, J., Morrell, M., Kippelen, B., & Peyghambarian, N. (1997). Highly efficient and bright organic electroluminescent devices with an aluminum cathode. *Applied Physics Letters*, 71(13), 1762-1764.
- Jou, J. H., Kumar, S., Agrawal, A., Li, T. H., & Sahoo, S. (2015). Approaches for fabricating high efficiency organic light emitting diodes. *Journal of Materials Chemistry C*, 3(13), 2974-3002.
- Kelleher, J. D., Mac Namee, B., & D'Arcy, A. (2015). Fundamentals of machine learning for predictive analytics. Cambridge, MA. The MIT Press.

- Kluyver, T., Ragan-Kelley, B., Perez, F., Granger, B., Bussonnier, M., Frederic, J., ... Team, J. D. (2016). Jupyter notebooks: A publishing format for reproducible computational workflows. In *Positioning and Power in Academic Publishing: Players, Agents and Agendas* (pp. 87-90). Washington, DC. ISO Press.
- Kuik, M., Koster, L. J. A., Wetzelaer, G. A. H., & Blom, P. W. M. (2011). Trap-assisted recombination in disordered organic semiconductors. *Physical Review Letters*, *107*(25), Article#256805.
- Lakowicz, J. R. (2013). Principles of fluorescence spectroscopy: Springer Science & Business Media.
- Lee, H. W., Lee, S. E., Lee, J. W., Sun, Y., Yang, H. J., Lee, S., ... Kim, Y. K. (2014). Effect of ITO-free Ni/Ag/Ni electrode on flexible blue phosphorescent organic light-emitting diodes. In *2014 21st International Workshop on Active-Matrix Flatpanel Displays and Devices (AM-FPD)* (pp. 261-262). Kyoto, Japan. IEEE.
- Leung, M.-k., Yang, C.-C., Lee, J.-H., Tsai, H.-H., Lin, C.-F., Huang, C.-Y., ... Chiu, C.-F. (2007). The unusual electrochemical and photophysical behavior of 2, 2'-bis (1, 3, 4-oxadiazol-2-yl) biphenyls, effective electron transport hosts for phosphorescent organic light emitting diodes. *Organic Letters*, *9*(2), 235-238.
- Maaten, L. v. d., & Hinton, G. (2008). Visualizing data using t-SNE. *Journal of Machine Learning Research*, *9*, 2579-2605.
- McKinney, W. (2010). Data structures for statistical computing in python. In *Proceedings of the 9th Python in Science Conference* (Vol. 445, pp. 51-56). Austin, TX.
- Millman, K. J., & Aivazis, M. (2011). Python for Scientists and Engineers. *Computing in Science & Engineering*, *13*(2), 9-12.
- Nicolai, H. T., Kuik, M., Wetzelaer, G. A. H., de Boer, B., Campbell, C., Risko, C., ... Blom, P. W. M. (2012). Unification of trap-limited electron transport in semiconducting polymers. *Nature Materials*, *11*(10), 882-887.
- Oliphant, T. E. (2007). Python for scientific computing. *Computing in Science & Engineering*, *9*(3), 10-20.
- Park, J.-S., Chae, H., Chung, H. K., & Lee, S. I. (2011). Thin film encapsulation for flexible AM-OLED: a review. *Semiconductor Science and Technology*, *26*(3), Article#034001.
- Park, S.-R., Kim, S.-M., Kang, J.-H., Lee, J.-H., & Suh, M. C. (2017). Bipolar host materials with carbazole and dipyrindylamine groups showing high triplet energy for blue phosphorescent organic light emitting diodes. *Dyes and Pigments*, *141*, 217-224.
- Pedregosa, F., Varoquaux, G., Gramfort, A., Michel, V., Thirion, B., Grisel, O., ... Dubourg, V. (2011). Scikit-learn: Machine learning in Python. *Journal of Machine Learning Research*, *12*, 2825-2830.

- Schwartz, G., Reineke, S., Rosenow, T. C., Walzer, K., & Leo, K. (2009). Triplet harvesting in hybrid white organic Light - Emitting diodes. *Advanced Functional Materials*, 19(9), 1319-1333.
- Scott, J. C., & Malliaras, G. G. (1999). The chemistry, physics and engineering of organic light - emitting diodes. In *Semiconducting Polymers* (pp. 411-461). Weinheim. Wiley-VCH
- Shinar, J., & Savvateev, V. (2004). Introduction to organic light-emitting devices. In *Organic Light-Emitting Devices* (pp. 1-41). New York, NY. Springer.
- Shirota, Y., & Kageyama, H. (2007). Charge carrier transporting molecular materials and their applications in devices. *Chemical reviews*, 107(4), 953-1010.
- Singh, S., & Gupta, P. (2014). Comparative study ID3, cart and C4. 5 decision tree algorithm: A survey. *International Journal of Advanced Information Science and Technology (IJAIST)*, 27(27), 97-103.
- Song, W., & Lee, J. Y. (2017). Degradation mechanism and lifetime improvement strategy for blue phosphorescent organic light-emitting diodes. *Advanced Optical Materials*, 5(9), Article#1600901.
- Tang, C. W., & Vanslyke, S. A. (1987). Organic electroluminescent diodes. *Applied Physics Letters*, 51(12), 913-915.
- Tao, Y., Yang, C., & Qin, J. (2011). Organic host materials for phosphorescent organic light-emitting diodes. *Chemical Society Reviews*, 40(5), 2943-2970.
- Tokito, S., Iijima, T., Suzuri, Y., Kita, H., Tsuzuki, T., & Sato, F. (2003). Confinement of triplet energy on phosphorescent molecules for highly-efficient organic blue-light-emitting devices. *Applied Physics Letters*, 83(3), 569-571.
- Van Der Walt, S., Colbert, S. C., & Varoquaux, G. (2011). The NumPy array: A structure for efficient numerical computation. *Computing in Science & Engineering*, 13(2), 22.
- VanderPlas, J. (2016). Python data science handbook: Essential tools for working with data. O'Reilly Media, Inc.
- Vincett, P., Barlow, W., Hann, R., & Roberts, G. (1982). Electrical conduction and low voltage blue electroluminescence in vacuum-deposited organic films. *Thin Solid Films*, 94(2), 171-183.
- Wang, G.-F., Tao, X.-M., & Wang, R.-X. (2008). Fabrication and characterization of OLEDs using PEDOT: PSS and MWCNT nanocomposites. *Composites Science and Technology*, 68(14), 2837-2841.
- Wei, M.-K., Lin, C.-W., Yang, C.-C., Kiang, Y.-W., Lee, J.-H., & Lin, H.-Y. (2010). Emission characteristics of organic light-emitting diodes and organic thin-films with planar and corrugated structures. *International Journal of Molecular Sciences*, 11(4), 1527-1545.

- Woon, K. L., Hasan, Z. A., Ong, B. K., Ariffin, A., Griniene, R., Grigalevicius, S., & Chen, S. A. (2015). Triplet states and energy back transfer of carbazole derivatives. *RSC Advances*, 5(74), 59960-59969.
- Wu, C., Wu, C., Sturm, J., & Kahn, A. (1997). Surface modification of indium tin oxide by plasma treatment: An effective method to improve the efficiency, brightness, and reliability of organic light emitting devices. *Applied Physics Letters*, 70(11), 1348-1350.
- Xu, H., Chen, R., Sun, Q., Lai, W., Su, Q., Huang, W., & Liu, X. (2014). Recent progress in metal-organic complexes for optoelectronic applications. *Chemical Society Reviews*, 43(10), 3259-3302.
- Yersin, H. (2008). Highly efficient OLEDs with phosphorescent materials. Weinheim. Wiley-VCH.
- Yin, X., Sun, H., Zeng, W., Xiang, Y., Zhou, T., Ma, D., & Yang, C. (2016). Manipulating the LUMO distribution of quinoxaline-containing architectures to design electron transport materials: Efficient blue phosphorescent organic light-emitting diodes. *Organic Electronics*, 37, 439-447.
- Zhou, Y. C., Zhou, J., Zhao, J. M., Zhang, S. T., Zhan, Y. Q., Wang, X. Z., ... Hou, X. Y. (2006). Optimal thickness of hole transport layer in doped OLEDs. *Applied Physics a-Materials Science & Processing*, 83(3), 465-468.
- Zhu, M. R., & Yang, C. L. (2013). Blue fluorescent emitters: design tactics and applications in organic light-emitting diodes. *Chemical Society Reviews*, 42(12), 4963-4976.

LIST OF PUBLICATIONS AND PAPERS PRESENTED

Publication

1. **Janai, M. A. B.**, Woon, K. L., & Chan, C. S. (2018). Design of efficient blue phosphorescent bottom emitting light emitting diodes by machine learning approach. *Organic Electronics*, 63, 257-266.

University of Malaya